GENERAL INFORMATION

Welcome

Welcome to the Fall 2006 Meeting of the Four Corners Section of the American Physical Society and the Zone 15 Meeting of the Society of Physics Students. We hope you enjoy your stay in Logan.

Information and Registration Desk

The registration desk will remain open for the duration of the conference. Feel free to ask any staff members or members of the local organizing committee for help.

Parking

Parking is available on Friday in the Parking Terrace (for a fee), which is located north of the Campus Inn. Most lots are open and free after 3:45 on Friday and all day Saturday. Parking regulations are strictly enforced.

Internet Access

Wireless internet access is available in the Eccles Conference Center during the conference. Please inquire at the registration desk for a instructions on gaining access.

Oral Sessions

Presenters, please make sure that you computer will work smoothly with the projector; do this during the break time between sessions. Any time lost in setting up you computer will count towards the time allotted for your talk.

Chairs, please be available during the break time before your session to help the speakers check out the interfacing of their computers with the projectors.

Poster Session

Presenters, please put you poster up at the beginning of the conference. The official time for the poster session is 5:30 pm – 6:30 pm on Friday, but feel free to discuss your poster anytime during the conference, especially during the coffee breaks on Friday and Saturday.

Student Competition

Students, if you registered online and you are the first author on a presentation, then you are automatically entered into the student competition for the best student presentations. Presentation of the awards will take place at the end of the conference in Session SA.

Judges, immediately after each session that you judge, please return your forms for that session to either Eric Held, J. R. Dennison, or Andrea Palounek.

ACKNOWLEDGMENTS

Financial Contributors – Thanks!

Utah State University Physics Department
Utah State University College of Science
Utah State University Space Dynamics Laboratory
Society of Physics Students

Local Organizing Committee

Mark Riffe (USU), Local Committee Chair
Jan Marie Anderson (USU Student)
J. R. Dennison (USU)
Eric Held (USU)
David Peak (USU)
Cade Perkins (USU Student)
T.-C. Shen (USU)
Jan Sojka (USU)
Mike Taylor (USU)
Charlie Torre (USU)
Jodie Tvedtnes (USU Student)

Feedback

Feel free to let us know what you liked and what you didn't like about the conference. Contact us at riffe@cc.usu.edu.

EATING ESTABLISHMENTS

On Campus

The Taggert Student Center houses two eating establishments that are available to conference participants for lunch. The HUB food court is located in the SE corner of the ground floor. The Skyroom is located on the top floor, near the center of the building.

The Library houses the Quadside Cafe, which is open from 7:00 am - 5:00 pm on Fridays and 12:00 pm - 5:00pm on Saturdays. It is located on the east side of the library (which is east of the Eccles Conference Center).

Off Campus

Logan has a number of eateries. None are within a short walking distance of the conference site. The highest densities of restaurants are along North Main street and along East 1400 N.

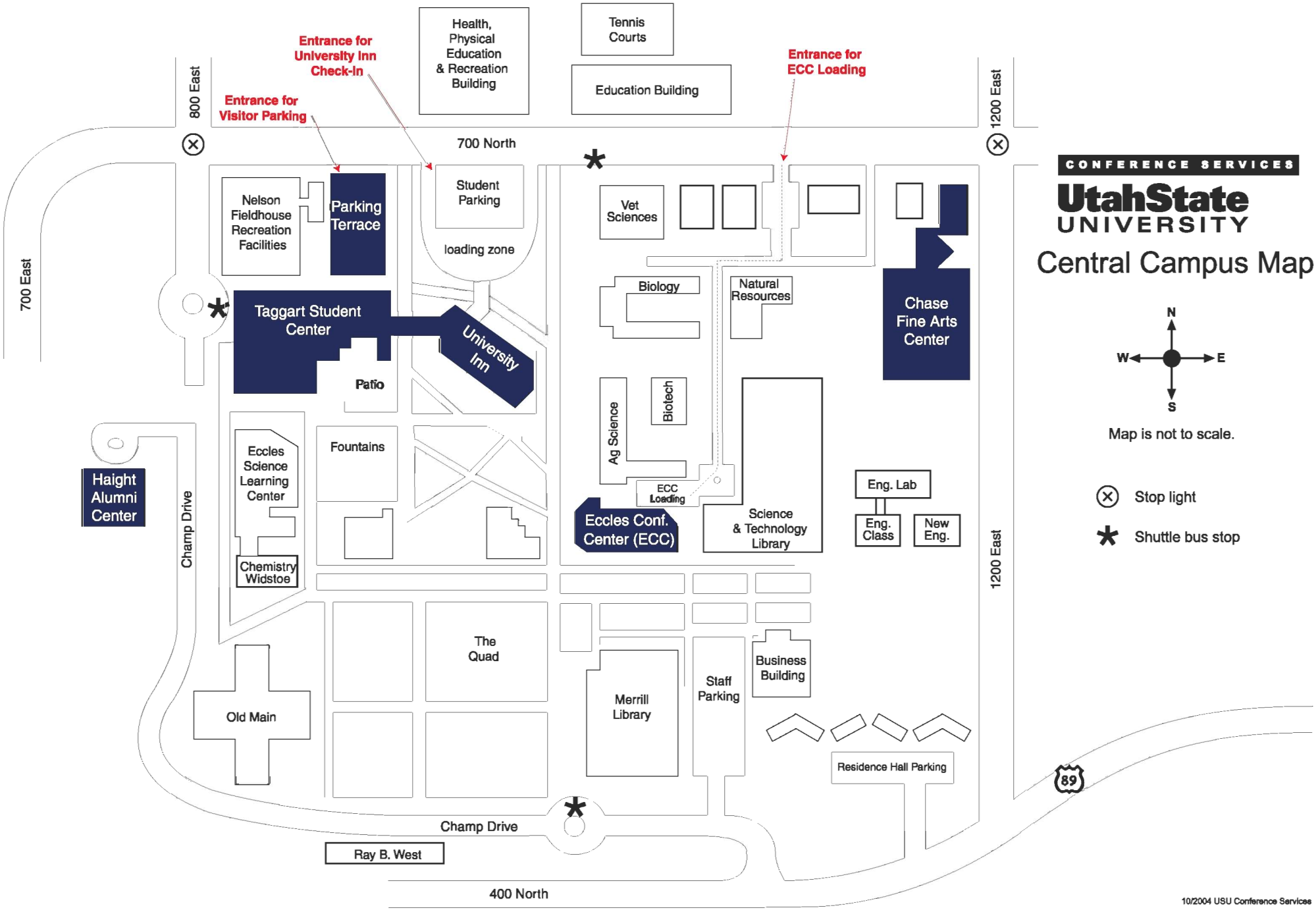

CONFERENCE SERVICES

UtahState UNIVERSITY

Central Campus Map

10/2004 USU Conference Services

SPS EVENTS

Pizza Reception and USU Physics Department Open House

On Thursday evening a pizza reception and open house of the USU physics Department will take place in the SER Building, which houses the Physics Department.

SPS Friday Luncheon

A luncheon sponsored by SPS will be provided for conference attendees on Friday at 12:15. At 12:45 Gary White, the National SPS Director, will talk about careers in physics.

Graduate School Fair

There will be an opportunity to talk with representatives from Graduate Programs in the Four Corners region during Friday's poster session, 5:30 pm - 6:30 pm.

Amusement Park Physics

The USU SPS Chapter invites all SPS attendees to join them at the local S and S Power amusement park on Saturday from 2:00 to 5:00 pm, after the conference. S and S Power has invented and built numerous rides for amusement parks all over the world, including the Space Shot on top of the Stratosphere Tower in Las Vegas. One of the coolest rides at the park entails a 4 second free fall!

For students registered for the conference the entry fee is 15 dollars for the first 40 who sign up (and 25 dollars thereafter). Both rates are quite a deal since a half day pass to the park is generally 35 dollars. This includes access to the Rock Wall, Slick Track, Go Cart Track, Screaming Swing, Sonic Boom, Sky Coaster, Soft Play, and the Carousel.

Student Introductions

Throughout the conference Utah-State-University SPS-Chapter members will be making brief introductions of the invited speakers.

SPS Chapter Summaries

The following five pages summarize the recent or upcoming activities of five of the Zone 15 SPS Chapters. The chapters are from Weber State University, Brigham Young University, Brigham Young University - Idaho, Idaho State Uiversity, and Utah State University.

Physics Club
Weber State University

PHYSICS DESTRUCTION DAY

One of our goals as a club is to help the student community understand that physics can be really fun. One of our activities is Physics Destruction Day. This could be called physics destruction/demo day but we noticed that more people are attracted to the word destruction and so we use it to help spark interest in people. This activity is bi-weekly and some of the things we have done include destruction by gravity i.e. we dropped pumpkins, watermelon, cantaloupe, and other fruit and vegetables that would explode on impact with the ground. We have also done destruction by solar energy using a large lens to focus sun light and melt copper and salt. We have also done the Diet Coke geyser. We have also entered the Ogden festival of trees.

PHYSICS CHRISTMAS TREES

Our club decorates a Christmas tree and the proceeds from its auction are given to charity. For this year we are considering "Christmas Tree on a Neutron Star" as our theme.

WHAT HAPPENS IN WENDOVER STAYS IN WENDOVER!

As a way of unwinding and socializing with our professors we go on our semesterly trip to Wendover to study statistics, enjoy a great meal, and socialize with one another.

ROOTBEER!

This year we are going to brew root beer and then make root beer floats with liquid nitrogen ice cream. We also participate in the Weber States Science Emphasis Week.

SPS 2005-2006
BYU Chapter

Our Chapter of SPS over the course of the 2005-2006 school year has been very productive. We focused on trying to increase the participation and involvement in SPS we get from our fellow students. Previous years of SPS have not exactly excited the students. We took up the challenge of turning that all around. We had exciting activities every month. Some activities were just fun and food and some were great fun and awesome food. If you are looking for ideas for activities, some of the highlights were PALF (paper airplane golf), pi day, and liquid nitrogen party. We set up holes around the building and let them make paper airplanes and have at it. For pi day (March 14), we had a **pie eating contest**. For our liquid nitrogen party, we had a good vat of the good stuff and let students bring stuff to smash with a hammer after freezing it. Our activities were so fun and so popular that by the end of the year, we had hundreds of students at each and every activity.

Another aspect of SPS that we have been pushing is Outreaches. These are activities where SPS members volunteer to visit classrooms and assemblies at various schools (K-12) with **physics demos** and explain the physics behind them to the kids. Some of our demos were getting old and we got an outreach grant of $300 to purchase/create new demos to keep the students entertained and get them excited about science. We visited dozens of schools in the area and got positive feedback and interest must have been instilled in the minds of the little students.

BYU-Idaho SPS and Fall Kick-Off Report

The BYU-Idaho Society of Physics Student Chapter has had a moderately active year. We hosted the AAPT UT/ID section meeting here in Rexburg Last Spring and helped coordinate the conference. We had a fun activity shooting off model rockets (see photo below) and also helped with the First Annual Spring Undergraduate Research Conference in March.

We also just held our Fall Kick-Off and elections meeting September 13, 2006. About 20 people attended and enjoyed refreshments, some examples of Physics bloopers in the movies, and planned activities for the year. These include: A trip Oct. 5-7 to the APS Four-Corners section meeting and SPS Zone 15 meeting in Logan, UT; A November activity "What not to do with your mother's microwave" (see http://www.byui.edu/scroll/20051025/front1.html for a review of the last time we did this); A February activity volunteering to man the registration desk at the 2nd Annual BYU-Idaho Spring Undergraduate Research Conference; and a celebration of Pi Day and Einstein's Birthday in March. We may also take a trip to the AAPT UT/ID section meeting in Logan the end of March.

The new BYU-I SPS section officers for 2006-2007 include:
Pres: Cameron Sanders
VP: Berkley Starks
Sec. Mike Matusek
Treas: Carl Grafe
Activities Chair: Brett Mattison
Asst. Act. Chair: Brandon Kuhns
Membership Chair: Candice Humpherys
Public Relations: David Stewart

-Dr. Brian A. Pyper
BYU-I Physics Dept.
SPS Advisor
pyperb@byui.edu

ISU SPS Activities, Sept. '05 - May '06

Designed a fire-breathing Bengal tiger (ISU's mascot) for the September Home Coming parade, but the Pocatello Fire Marshall thought it was too scary.

Built a giant trebuchet with a 10 m throwing arm for an annual Punkin' Chukn' Competition held at Snake River High School in Blackfoot on Oct. 31. Our device was by far the largest towed onto the field af battle that brisk morning. We had the competition shaking in their boots, until the main arm of our terror spectacularly shattered during the first shot. We are rebuilding our engine of destruction, and this year we'll show 'em!

Once again our Haunted Physics Lab was a success. On Oct. 28 in our Student Union, and on Oct. 31 at a local school, our club entertained over 300 kids and parents with spooky science fun. We had 25 interactive exhibits, mostly on optics and electromagnetism. We used parabolic mirrors to produce a vampire in front a flat mirror - no reflection! We had holograms, in inverted "Einstein Alive!" mask, a candle burning underwater, a talking disembodied head (done with mirrors), a laser light show, cylindrical mirrors with hidden messages, and a spectacular Pepper's Ghost display. We had Tesla coils, a Van de Graaff, vortex cannons, and flying bats to illustrate centripital force. We had lots of black lights, phosphorescent stuff, fiber optics, and strobe lights. Trick-or-treaters used a phosphorescent screen and a flash to walk away from their own shadow, and used a magic wand and our own persistence of vision to make a ghost appear out of thin air. Setting stuff up twice was a pain, but much fun was had by all.

We had a big post-Punkin' Chunk'n post-Halloween party, then did nothing for at least a month.

We put on a giant Physics Spectacular on April 8, with two physics demo shows, hovercraft rides, and a chocolate Easter Egg hunt for the kids, with the eggs deployed via potato gun. Twelve club members took turns performing demos to packed crowds. About 250 people attended.

Throughout the year, members assisted Dr. Shropshire in his Physics on the Road program, visiting 58 K-12 schools for demo shows. Sixteen of these visits were to high schools to blow stuff up, set stuff on fire, and to talk to folks about studying physics.

Utah State University Chapter of SPS

During the 2005-06 school year our SPS Chapter was involved in several activities, ranging from service projects to tours.

Our Year-Opening Social was a pizza party/physics lab tour for which we had a great turnout from both faculty and students.

We volunteered at the USU Physics Day at the Lagoon Amusement Park. Physics Day at Lagoon is an annual event that involves over 4,000 students in grades 7-12 from schools in Utah, Idaho, Wyoming, and Nevada engaging in various competitions—including measuring ride accelerations (left) and Physics Bowl. This year we helped edit the hundreds of Physics Bowl questions and run the event.

As a modestly successful fundraiser, we produced the Physics Department's first ever "yearbook," a CD (right) with photos of almost all of our undergraduate and graduate majors plus other memorabilia.

On two separate occasions we visited the University's Bear Lake Observatory, performing cleanup and maintenance on the building (left).

Finally, for tours, our group visited Dupont Holographics and Campbell Scientific (right), local scientific instrumentation companies.

For the coming year we are starting a Mentoring Program for freshmen and transfer students newly entering the Physics Department at USU and we have just begun a GRE preparation study group. Our plans also include involvement in school-wide club recruitment activities, going on more tours, and to once again volunteer for Physics Day. And, of course, we look forward to hosting the Zone 15 SPS meeting in October.

Epitome – Friday, October 6, 2006

8:00AM

WE: Welcome
Eccles Conference Center Room 216
Chair: Mark Riffe, Utah State University

8:15AM

A1: Physics in the Four Corners Region I
Eccles Conference Center Room 216
Chair: Bruce Doak, Arizona State University
Invited Speakers: Solomon, Shinn, Turner

10:00AM

Coffee Break – Third Floor Hallway

10:30AM

B1 Computational Physics Symposium
Eccles Conference Center Room 216
Chair: Eric Held, Utah State University
Invited Speakers: Bhattacharya, Cary, Plimpton

B2 Lasers, Optics, and Spectroscopy
Eccles Conference Center Room 205/207
Chair: William E. Evenson, Utah Valley State College

B3 Condensed Matter Structure and Spin
Eccles Conference Center Room 201/203
Chair: Dieter Hochheimer, Colorado State University

B4 Astrophysics
Eccles Conference Center Room 305
Chair: Tom Tierney, Los Alamos National Laboratory

12:15PM

SPS Sponsored Luncheon – Third Floor Hallway

12:45PM

C1 SPS Luncheon Presentation
Eccles Conference Center Room 216
Chair: Jodie Tvedtnes, Utah State University
Invited Speaker: White

1:30PM

D1 Thin Films and Quantum Dots
Eccles Conference Center Room 216
Chair: Heinz Nakotte, New Mexico State University

D2 Bio-related Physics
Eccles Conference Center Room 205/207
Chair: Jean Francois Van Huele, Brigham Young U.
Invited Speaker: Doak

D3 Plasmas and Fusion
Eccles Conference Center Room 201/203
Chair: Ross Spencer, Brigham Young University

D4 General Physics and Physics Education
Eccles Conference Center Room 305
Chair: Brian Pyper, Brigham Young University-Idaho

3:15PM

Coffee Break – Third Floor Hallway

3:45PM

E1 Physics in the Four Corners Region II
Eccles Conference Center Room 216
Chair: Bill Fairbank, Colorado State University
Invited Speakers: LeRoy, Lewandowski, Hochheimer

5:30PM

F1 Poster Session
Eccles Conference Center Third Floor Hallway
Chair: David Peak, Utah State University

6:30PM

Reception and Banquet
Copper Mill Restaurant, 55 N Main, Logan

8:30PM

G1 Banquet Talk
Copper Mill Restaurant, 55 N Main, Logan
Chair: Jan Sojka, Utah State University
Invited Speaker: Cleave

Epitome – Saturday, October 7, 2006

8:30AM

H1: Nanoscale Physics
Eccles Conference Center Room 216
Chair: J.R. Dennison, Utah State University
Invited Speaker: Gerton

H2 Condensed Matter Electronic Properties
Eccles Conference Center Room 205/207
Chair: T.C. Shen, Utah State University

H3 Applied Physics and Spectroscopy
Eccles Conference Center Room 201/203
Chair: Charles Durfee, Colorado School of Mines

H4 Fields and General Theory
Eccles Conference Center Room 305
Chair: Charles Torre, Utah State University

H5 Atmospheric and Nuclear Physics
Eccles Conference Center Room 309
Chair: Andrea Palounek, Los Alamos National Laboratory

10:15AM

Coffee Break – Third Floor Hallway

10:45AM

I1 The Final Frontier?
Eccles Conference Center Room 216
Chair: Keith Dienes, University of Arizona
Invited Speakers: Torre, Thomas, Murayama

12:35AM

SA Student Awards
Eccles Conference Center Room 216
Chair: Keith Dienes, University of Arizona

Session WE: Welcome

Eccles Conference Center - Room 216
Friday, October 6, 2006 8:15AM - 8:30AM
Chair: Mark Riffe, Utah State University

Opening remarks and last minute details for conference participants.

Session A1: Physics in the Four Corners Region I

Eccles Conference Center - Room 216
Friday, October 6, 2006 8:15AM - 10:03AM
Chair: Bruce Doak, Arizona State University
SPS Student Introductions: Hema Karnam, Robert Ream, Tamara Jeppsen

(8:15) A1.00001: Observations and Modeling of Space Weather Impacts on the Earth
Invited Speaker: Stanley C. Solomon

"Space weather" refers to conditions in the solar wind, magnetosphere, ionosphere, and upper atmosphere, that influence space-borne and ground-based technological systems and can endanger human space exploration. These effects are caused by variations in solar photon and particle radiation due to flares and coronal mass ejections, and changes in the solar/interplanetary magnetic field, that impact the magnetosphere and ionosphere. Space weather can initiate satellite failures, interfere with radio communications, cause navigation errors, disrupt electrical power distribution systems, and expose astronauts to dangerous levels of radiation. Mitigation requires both a better understanding of the space environment, and developing the ability to forecast conditions in space. The development of first-principles numerical models of the solar-terrestrial system gives us insight into the causes and nature of these phenomena, and holds the promise of ultimately being able to acquire a short-term predictive capability for some of them. This presentation will describe what we do and don't understand about the basic physics behind space weather, discuss some of its aspects and effects, and describe the latest observational and modeling efforts

(8:51) A1.00002: Nanotechnology Integration
Invited Speaker: Neal Shinn

Interest in nanoscience – and derivative nanotechnologies – has grown explosively because of the perceived potential to beneficially impact almost every aspect of our lives. The remarkable scientific discoveries obtained by working at the molecular length scale will disappoint humankind if they cannot be exploited by integration into technologies providing unprecedented functionality and performance. To bridge the gap between nanoscience discovery and technology, we must tackle the intrinsic science challenges of integration. This talk examines three such challenges: the fundamental limits and principles for the use and integration of nanoscale structures to detect, transfer, and harvest energy with extreme efficiency or sensitivity; the principles of transduction events in natural systems and how these may be incorporated into artificial systems to convert single molecular events into large scale responses; and the collective properties of composite nanoscale systems that cannot be predicted in terms of the individual constituents. Success in solving such nanoscience integration challenges will change not only what is expected of future technologies, but also the way in which they accomplish ever more complicated tasks.

(9:27) A1.00003: The Sustainable Hydrogen Economy: Addressing the Challenges Ahead
Invited Speaker: John A. Turner

It is rapidly becoming apparent that energy is one of the most important issues facing our world today; in fact, in today's society energy is as important as food and water. Humankind finds itself faced the challenge of how to continue to power society, particularly in the face of the rapidly growing economies of emerging nations like India and China, and yet answer questions of sustainability, energy security, geopolitics and global environment. One of the major issues facing America and most other countries in the world is how to supply a transportation fuel, an energy carrier to replace gasoline. Hydrogen as an energy carrier, primarily derived from water, can address issues of sustainability, environmental emissions and energy security. The "Hydrogen Economy" then is the production of hydrogen, its distribution and utilization as an energy carrier. While the vision of a hydrogen economy has been around for over 130 years, the most recent push to use hydrogen as an energy carrier came as part of a US Presidential Initiative, announced in the 2003 State of the Union Address. It is important that we consider hydrogen in tandem with other technologies as an alternative to the once-abundant hydrocarbon resources on which our society depends. This talk will introduce sustainable energy systems, including fuel cell technology and discuss the vision, the barriers and possible pathways for the production and implementation of hydrogen into the energy infrastructure.

Session B1: Computational Physics Symposium

Eccles Conference Center - Room 216
Friday, October 6, 2006 10:30AM - 12:18AM
Chair: Eric Held, Utah State University
SPS Student Introductions: Mukta Sharma, John James, Michael Addae-Kagyah

(10:30) B1.00001: Computational Approaches to Viral Evolution and Rational Vaccine Design
Invited Speaker: Tanmoy Bhattacharya

Viral pandemics, including HIV, are a major health concern across the world. Experimental techniques available today have uncovered a great wealth of information about how these viruses infect, grow, and cause disease; as well as how our body attempts to defend itself against them. Nevertheless, due to the high variability and fast evolution of many of these viruses, the traditional method of developing vaccines by presenting a heuristically chosen strain to the body fails and an effective intervention strategy still eludes us. A large amount of carefully curated genomic data on a number of these viruses are now available, often annotated with disease and immunological context. The availability of parallel computers has now made it possible to carry out a systematic analysis of this data within an evolutionary framework. I will describe, as an example, how computations on such data has allowed us to understand the origins and diversification of HIV, the causative agent of AIDS. On the practical side, computations on the same data is now being used to inform choice or defign of optimal vaccine strains.

(11:06) B1.00002: Recent discoveries from massive computation in beam physics
Invited Speaker: John Cary

In the last decade, computational beam physics, the study of the generation, propagation, and dynamics of charged particle beams, has moved from workstation computing to the use of massive parallelism, in which the power of hundreds to thousands of cpus are simultaneously harnessed to solve problems at the forefront of beam and accelerator science. The result has been multiple discoveries, including the prediction of the generation of GeV beams from lasers interacting with only a few centimeters of plasma. The field has gained in importance and prediction capability to where no accelerator will be built without extensive prior analysis of designs by computation in order to predict performance. This is especially important in the design of large accelerators, like the proposed International Linear Collider, which will have two 17 km long beams and has a cost estimated to be of the order of $10B. This talk will summarize the recent advances in capability, the underlying computational technology, and some of the recent discoveries in this area.

(11:42) B1.00003: Simulating Biological Cells
Invited Speaker: Steve Plimpton

Cells interact with their environment via a cascade of biochemical reactions that invoke a signaling, metabolic, or regulatory response. The properties of these reaction networks can be modeled at various levels of detail from continuum to stochastic, and steady-state to kinetic. Our group (and others) have been developing tools that attempt to simulate these networks in cellular geometries with spatio-temporal detail. In our model a single particle represents a protein, complex, or other biomolecule. Membranes and cellular compartments are represented as idealized or triangulated surfaces. Particles diffuse via 3d Brownian motion within the cytoplasm, or in 2d on membrane surfaces. When particles are near each other, they interact in accord with Monte Carlo rules to perform biochemical reactions which represent complex formation, dissociation events, ligand binding, etc. In this talk, I'll describe the reaction algorithms we use and the underlying physics they attempt to capture. I'll illustrate the effects stochasticity and spatial organization have on biochemical networks at the cellular scale and show some simple examples of how such models can address biological questions. This is an emerging field of simulation, so there are many issues still to be addressed, but the eventual goal is to enable whole-cell models of protein networks with realistic numbers of biomolecules.

Session B2: Lasers, Optics, and Spectroscopy

Eccles Conference Center - Room 205/207
Friday, October 6, 2006 10:30AM - 12:18AM
Chair: William E. Evenson, Utah Valley State College

(10:30) B2.00001: Development of a kHz-repetition rate TW ultrafast amplifier

Charles Durfee , Thomas Planchon , Sudipta Bera , Jeff Field , Daniel Adams , Colby Childress , Jeff Squier – We have developed a 2 stage amplifier for ultrafast that will deliver 20mJ, 20fs laser pulses at a repetition rate of 1kHz. The novel power amplifier is pumped by up to 100W from 4 pump lasers, necessitating cryogenic cooling of the amplifier crystal. In collaboration with Abbess Instruments, we have designed a liquid nitrogen cooled cryostat that gives a temperature rise of less than 2K with a 100W thermal load. We have also developed a high resolution, high efficiency, temporal pulse shaper that will be integrated in the system. We will present our results on using the third-harmonic signal from a glass slide in the focus to optimize the wavefront from a deformable mirror and to fully characterize the temporal profile of the output pulse. This system is already being used for micromachining studies. In the near future it will be used for the generation of high flux hard x-rays for imaging and ultrafast x-ray diffraction.

(10:42) B2.00002: Direct Observation of Laser Filamentation in High-Order Harmonic Generation

Gavin Giraud , John Painter , Nicole Brimhall , Mark Adams , Nathan Powers , Eric Christiansen , Matt Turner , Michael Ware , Justin Peatross – We investigate the spatial evolution of a laser pulse used to generate high-order harmonics (orders ranging from 45-91) in a semi-infinite helium-filled gas cell. The 5 mJ, 30 fs laser pulses experience elongated focusing with two distinct waists when focused with f/125 optics in 80 torr of helium. An extended phase matching for the generation of harmonics occurs in the region between the double foci of the laser, where the laser beam changes from diverging to converging.

(10:54) B2.00003: The Application of High-Order Harmonics to Extreme Ultraviolet Polarimetry

Nicole Brimhall , John Painter , Matthew Turner , R. Steven Turley , Michael Ware , Justin Peatross – We report on the construction of an extreme ultraviolet (EUV) polarimeter based on high-order harmonic generation for characterizing optical surfaces from 8-62 nm. High harmonics as an EUV source are advantageous in that they are polarized (linear, same as laser) and measurements of several wavelengths of light can be made simultaneously. Although not as bright as a synchrotron source, the flux of EUV light is 30,000 times that of a commonly used plasma source. We have demonstrated the feasibility of this project with a simple prototype instrument, which measured the reflectance of samples from 30 nm to 62 nm. The prototype demonstrated that sensitivity is sufficient for measuring reflectances as low as 0.5%. The full instrument employs extensive scanning mobility as opposed to the fixed angle and fixed wavelength range of our earlier prototype. This project represents an authentic 'work-horse' application for high-order harmonics, as opposed to merely demonstrating proof of concept.

(11:06) B2.00004: Advantages of a Grazing Incidence Monochromator in the Extreme Ultraviolet

Sarah Barton , R. Steven Turley – One of the main goals of the BYU Thin Films group is to find optical constants for materials in the Extreme Ultraviolet. This is accomplished by taking reflection and transmission measurements. The addition of a Grazing Incidence Monochromator to our current system allows us to take reflectance measurements at wavelengths currently unavailable on the Normal Incidence Monochromator (Monarch).

(11:18) B2.00005: Oxidation Effects on the Optical Constants of Heavy Metals

Amy Grigg , Steve Turley – Applications for high-energy and extreme ultraviolet light are increasing everywhere in todays technological world. As a result, the need for understanding how light interacts with materials in this energy range of light is also increasing. This study examines a method for determining the optical constants of materials based on reflectance and transmission measurements, taking into account oxidation gradients of the material. The method of x-ray photoelectron spectroscopy rastering is found to be the best method for determining molecular composition gradients.

(11:30) B2.00006: From Whence Come the Electrons

Jonathan Abbott , J.R. Dennison , Jason Kite , R.C. Hoffmann , Rob Davies – Measuring the electron emission energy spectrum from a material yields a similar curve regardless of the incident energy source, whether it is electrons, ions, photons (photoemission), or even thermal energy (thermionic emission). When measuring the spectrum for electron induced electron emission, there is a question of whether it is possible to distinguish the electrons originating from the beam from those originating inside the material. We discuss the limits of the conventional boundary of 50 eV between the electrons originating from the material (secondary electrons) and those originating from the primary beam (backscattered electrons). We present experimental results suggesting a more realistic boundary at the observed minimum in the emission spectrum. We also show that simple analysis of emission spectra of biased conducting samples (and charged insulating samples) can distinguish

between these two populations.

(11:42)B2.00007: The Emission Angle and Incident Energy Dependence of the Boundary between Secondary and Backscattered Electrons

J.R. Dennison , Jason Kite – A more realistic boundary to separate the electrons originating from the sample (secondary electrons) and those originating from the primary beam (backscattered electrons) in electron-induced electron emission spectra is the observed minimum in the emission spectrum. We present measurements of the emission spectra of polycrystalline Au over a range of incident energies from 100 eV $< E_b <$ 2500 eV, as a function of emission angle and energy, E_b. The dependence of the position of Emin and its associated yield intensity are investigated in terms of E_b and emission angle. Emin is roughly constant at $\sim$45% of E_b, but does show some more complex dependence on E_b. No significant emission angle dependence of E_{min} is evident. The emission spectral intensity at E_{min}, N(E_{min}), decreases with increasing emission angle, and scales approximately as a Lambert law proportional to the cosine of the emission angle. Finally, we discuss the effect of choosing this more realistic value to separate secondary and backscattered electrons on the secondary and backscattered yield values.

(11:54) B2.00008: Measuring Auger Signatures Using a Rotatable, High-Resolution Retarding Field Analyzer Faraday Cup Detector

Jason Kite , J.R. Dennison – Single event energy losses of electron scattering have been observed in the angle- and energy-resolved electron emission spectra. The surface sensitive Auger signature is commonly used to characterize sample quality and determine surface species via their emission energy signature. Auger measurements are usually accomplished with a lock-in amplifier and electrostatic analyzer or LEED-style retarding field analyzer. Our measurements confirm that Auger peaks can also be measured with a simple retarding field analyzer Faraday cup detector. Design details and sample measurements are presented. The signature Auger peaks measured on polycrystalline Au of the MNN transitions, at 1720 eV and 2030 eV, compare very well with those in the literature. Peak dependence on incident energy and emission angle are also discussed. This work is sponsored by the NASA Space Environments and Effects Program.

(12:06) B2.00009: Optimized controller design for an ECDL locked to at optical cavity

James Archibald , Brian Neyenhuis , Matthew Washburn , W. Sam Weyerman , Sean Warnick , Dallin Durfee – We have performed a study of optimized feedback control of an external-cavity diode laser (ECDL) locked to a high-finesse optical cavity. We have measured the response of the laser to current modulation and developed a mathematical model of our laser. Using this model, we have calculated optimized designs for the feedback controller which keeps the laser locked to the optical cavity.

Session B3: Condensed Matter Structure and Spin

Eccles Conference Center - Room 201/203
Friday, October 6, 2006 10:30AM - 12:30AM
Chair: Dieter Hochheimer, Colorado State University

(10:30) B3.00001: Domain Growth Law Violations in a Compressible 2D Ising Model

Matthew Wright – We carry out Monte Carlo studies of a compressible two-dimensional spin-exchange Ising model, varying the Hamiltonian to imitate the "unmixing" of different phase-separating binary alloys. The Ising model is frequently used to model the dynamics of binary alloys or magnetic materials by simulating annealing. Normally, the domain growth law is of the form R(t) = A + B t^n. It has been found that the expected value of n = 1/3 does not hold for models where elements with differing atomic sizes are mixed together. We discuss the implications of these results on real alloys.

(10:42) B3.00002: Magnetic Transitions In UCuSn

Karunakar Kothapalli , Sami El-Khatib , Farzana Nasreen , Ian Swainsson , Anna Llobet , Heinz Nakotte – We report on the dependence of the magnetic moment of UCuSn with temperature as determined from neutron-diffraction data that were obtained at Chalk River laboratory. In this compound, the magnetic moment is solely due to uranium. Using the Rietveld method, we were able to determine the magnitude and direction of the magnetic moments for various temperatures in the range 15 K to 70 K. Magnetic intensities are observed for temperatures below 62 K, and their temperature dependence shows that the magnetic moment increases with decreasing temperature. At around 31 K, there is a second anomaly in the temperature dependence of the moment, and this suggests that UCuSn exhibits two magnetic phase transitions at about 30 and 65 K.

(10:54) B3.00003: Muon spin resonance study on $UCu_{1.5}Sn_2$

Sami El-Khatib , G. Michael Kalvius , D.R. Noakes , E.J. Ansaldo , C.E. Stronach , E. Brück , A. Llobet , H. Nakotte – We report on muon spin relaxation measurements results on $UCu_{1.5}Sn_2$, which crystallizes in the $CaBe_2Ge_2$-type structure. Our analysis is consistent with collinear antiferromagnetic order with the transition temperature at 108±1K, which is in agreement with previous reports. The Brillouin-like behavior of the temperature dependence of magnetic order indicates localized $5f$ moments in this compound. Noticeable distortion in the magnetic structure occurring in the long-range order regime. The transition from paramagnetic region to the long-range ordered region has been explained by a model, which adopts the fast and slow relaxation rates.

(11:06) B3.00004: High-pressure Raman studies of both hcp phases of Ba.

Helmut Olijnyk , Satoshi Nakano , Kenichi Takemura – Both hcp high-pressure phases of Ba were sudied by Raman spectroscopy. Combining the Raman data with existing equation of state data, the pressure dependence of the elastic shear modulus C_{44} has been derived. The pressure shift of the E_{2g} phonon frequency is discussed in terms of elastic parameters. Though the pressure response of the observed phonon mode shows normal behaviour in both phases, more subtle differences can be traced back to differences in the interatomic interactions in both phases.

(11:18) B3.00005: Phase diagram of Ti metal at high pressure

Yahya Al Khatatbeh , Kanani Lee , Boris Kiefer – Using density-functional theory based ab-initio computations, we have investigated the hexagonal close-packed (hcp) and the hexagonal (ω) structures titanium (Ti), and find good agreement with experiment. The hcp phase yields an equation of state of a zero pressure volume V_0 = 17.37 (0.02) Å^3, an isothermal bulk modulus K_0= 111.9 (0.2) GPa, and its pressure derivative K_0' = 3.60 (0.02). Furthermore, the c/a ratio for both phases increases with increasing pressure. Additionally, the calculated transition pressure from hcp to ω phase compares well with the experimental results with the ω phase more stable than the hcp phase at pressures greater than $\sim$ 5 GPa.

(11:30) B3.00006: Temperature dependence of absorption and emission spectra of Ba in solid Ar

Brian Mong – Detection of a single Ba daughter from extremely rare Xe-136 $\beta\beta$ decay is an essential part of the EXO (Enriched Xenon Observatory) project. At CSU we have been working on detection methods in both solid and liquid Xenon. This talk will cover the recent progress we have made on detection of Ba in solid Argon and Xenon. The absorption and fluorescence verses temperature in solid Ar and has been measured. Two Ba sites have been observed in solid Ar; site B recovers from annealing above 20K while site A does not, it converts to Site B. Recent progress with the spectroscopy of Ba and Ba+ in solid Xe will also be discussed.

(11:42) B3.00007: Experimental evidence for the existence of eigenvalues of the time evolution operator governing the behavior of nuclear spins in solids

Steven Morgan , Brian Saam – The decay of nuclear magnetic resonance (NMR) signals in solids is an extremely difficult many-body problem with no complete solution. Utilizing frozen xenon polarized by spin-exchange optical pumping, we have observed the long-time behavior of the NMR signal decay for both free-

induction decay and spin (solid) echoes. The enhanced signal has allowed us to view the behavior of the decay for up to ∼10 decay constants. This has given us the opportunity to test a theory about this behavior which says that at after a few time constants, the signal should decay either with a simple exponential or a simple exponential modulated by a sinusoid. The reasoning for this is that the evolution of the density matrix follows from the action of its complete time evolution operator, and that its eigenvalues determine the evolution of the spin system. Evidence for this type of behavior has been seen in classical chaotic systems, but ours is the first experimental evidence for this behavior in a quantum system. This work has the potential to help elucidate the role of chaos in quantum systems.

(11:54) B3.00008: Propagator Methods in Spintronics applied to the Rashba Hamiltonian

Bailey Hsu , Jean-Francois Van Huele – In spintronics, the spin of the electrons is manipulated to create spin currents. New propagators are introduced in order to determine the evolution of the spin systems. Rashba potentials are considered in connection with the spin-orbit couplings in condensed matter systems. We calculate the propagator for the Rashba Hamiltonian $H = \frac{P^2}{2m} + \frac{\alpha}{\hbar}(\sigma_x P_y - \sigma_y P_x)$ and comment on how to deal with noncommuting operators.

(12:06) B3.00009: Obtaining an EELS Fingerprint for the Phases of Aluminum Oxide

Michael Tanner , David Cullen , Richard Vanfleet – The crystal structure of Al_2O_3 is found naturally in a number of different atomic arrangements or phases (more than seven have been confirmed). By heating $Al(OH)_3$ (gibbsite) to different temperature levels in the lab, we obtained the alpha, gamma, and kappa phases which we confirmed by diffraction analysis. We then investigated these samples using electron energy-loss spectroscopy (EELS) in order to obtain an EELS fingerprint for each phase. A unique EELS fingerprint would allow phase identification in nanometer scale regions that cannot be measured by other means. Initial results are promising that the different phases can be differentiated by EELS. Further work will expand these measurements to include all of the phases of Al_2O_3.

(12:18) B3.00010: Microstructural Constitutive Theory: Statistical Particulate Mechanics

Michael Webb–

Session B4: Astrophysics

Eccles Conference Center - Room 305
Friday, October 6, 2006 10:30AM - 11:54AM
Chair: Tom Tierney, Los Alamos National Laboratory

(10:30) B4.00001: Laboratory Nuclear Astrophysics or The universe as seen from underground.

John E. Ellsworth , Steven E. Jones , Shannon Walch , Matthew R. Nerdin – Our sun emits 380 yottawatt, yet the nuclear reactant energies producing that power are very low (1 keV). These energies are so low, that replication of such reactions in the laboratory produce rates that are nearly impossible to detect. Unlike the historical efforts to understand stellar processes by extrapolating down from higher energy beam experiments, there are efforts to study reactions using low energy reactants. To do so requires specialized equipment and environments. The results indicate the need to understand the Coulomb screening effects of condensed matter in these processes. An explanation for heat production in planetary cores may also follow.

(10:42) B4.00002: Low energy accelerator for studying laboratory nuclear astrophysics.

Matthew R. Nerdin , John E. Ellsworth , Steven E. Jones – We present progress on the development of research equipment to study laboratory nuclear astrophysics reactions by bombarding deuterided metallic targets with accelerated ions. This effort consists of constructing a low energy accelerator and the initial testing of specialized low-rate, neutron and charged-particle detectors.

(10:54) B4.00003: Photoevaporation of Clustered Minihalos by Primordial Stars

Joseph Smidt , Dan Whalen – The first primordial stars to form in the universe were extremely luminous objects that heavily influenced subsequent star formation in their vicinity. We run 1D and 3D simulations of minihalo evaporation by a Pop III star to ascertain whether its radiation promotes or quenches star formation in the halo. Preliminary results will be presented.

(11:06) B4.00004: Phase-space distribution of unbound dark matter near the Sun

Moqbil Alenazi , Paolo Gondolo – We resolve discrepancies in previous analyses of the flow of collisionless dark matter particles in the Sun's gravitational field. We determine the phase-space distribution of the flow both numerically, tracing particle trajectories back in time, and analytically, providing a simple correct relation between the velocity of particles at infinity and at the Earth. We use our results to produce sky maps of the distribution of arrival directions of dark matter particles on Earth at various times of the year. We assume various Maxwellian velocity distributions at infinity describing the standard dark halo and streams of dark matter. We illustrate the formation of a ring, analogous to the Einstein ring, when the Earth is directly downstream of the Sun.

(11:18) B4.00005: Characterizing lasers for cosmic ray "test beams" at the Pierre Auger Observatory

Shoji Komatsu , Lawrence Wiencke , Miguel Mostafa – The Pierre Auger Observatory located in western Argentina is studying extended air-shower produced by high energy cosmic rays using two detectors: a Fluorescence Detector and a Surface Detector. Because cosmic rays test beams are unavailable, laser test beams are used to measure properties of Fluorescence Detector. Optical signatures of extended air-shower and laser test beams have several similarities. This talk will discuss characterization of the laser test beams including polarization and their absolute photometric calibration.

(11:30) B4.00006: Surveying the TeV Sky with Milagro

Gary Walker – A wide field of view, high duty factor TeV gamma-ray observatory is essential for studying TeV astrophysical sources, because most of these sources are either highly variable or are extended. Milagro is such a TeV detector and has performed the deepest survey of the Northern hemisphere sky. In addition to detecting the Crab Nebula and Mrk 421, which are known TeV sources, Milagro has made the first detection of diffuse TeV emission from the Galactic plane. In addition, Milagro has discovered a new, extended source in the Galactic plane that is coincident with an EGRET unidentified source. Based on the success of Milagro, a second generation water Cherenkov gamma-ray observatory is planned which will give an increase in sensitivity of more than an order of magnitude.

(11:42) B4.00007: Monocular spectrum and the search for exotic events in the ultra high energy cosmic ray data of HiRes (The High Resolution Fly's Eye)

Douglas Rodriguez – The High Resolution Fly's Eye (HiRes) experiment consists of two fluorescence detectors in search of the highest energy cosmic rays. These extremely energetic events can have 100 million times more energy than the highest energy achievable at man-made accelerators. The original Fly's Eye experiment observed one event with energy of 3.2 x 10^{20} eV. When such cosmic rays arrive at the Earth, they interact with the nitrogen and other gases of the upper atmosphere, generating a shower of secondary particles which in turn produce ultra-violet fluorescence light that can be viewed by our detectors. The data, collected between 5/1997 and 4/2006, has been analyzed in both monocular and stereo formats to study the energy spectrum above $10^{17.5}$ eV, incident particle composition, and source direction (anisotropy). I am analyzing the data from one HiRes

site, HiRes-1, to produce a final monocular energy spectrum and to look for exotic events, particularly double showers. These are showers that could originate from one primary particle, but appear to the detectors as two separate coincident tracks. I will present this work as well as other uses for these analysis programs.

Session C1: SPS Luncheon Presentation

Eccles Conference Center - Room 216
Friday, October 6, 2006 12:45PM - 1:21PM
Chair: Jodie Tvedtnes, Utah State University
SPS Student Introduction: Jennifer Albretsen

(12:45) C1.00001: Secret Lives of the Hidden Physicists—from Spandex to Spintronics
Invited Speaker: Gary White

What is a physicist? A case is made for defining a physicist as anyone with a bachelor's degree (or higher) in physics. Under this definition, a large fraction of physicists are hidden, that is, they have left, or never belonged to, the traditional lot of Ph.D. academicians. Data from the Statistical Research Center at the American Institute of Physics and from a survey of members of the national physics honor society, Sigma Pi Sigma, show the vast array of actual career paths taken by physicists. From spandex to blackberries to bioinformatics to flight control to wind energy to spintronics, physicists can be found in nearly every job sector in some of the coolest and most farfetched careers imaginable.

Session D1: Thin Films and Quantum Dots

Eccles Conference Center - Room 216
Friday, October 6, 2006 1:30PM - 3:06PM
Chair: Heinz Nakotte, New Mexico State University

(1:30) D1.00001: The Effect of Voltage Ramp Rate on Dielectric Breakdown of Thin Film Polymers

Anthony Thomas , J. Dennison , Steve Hart , Ryan Hoffmann – When a sufficient electric field is placed across a dielectric material, electrical breakdown occurs. The field strength at which this occurs is referred to as the dielectric strength or electrostatic discharge (ESD) voltage. The dielectric strength of thin (25 μm to 250 μm) film polymer samples (low density polyethylene, Teflon, Kapton, Mylar, and other fluorocarbon polymers) have been measured by placing them between parallel plate electrodes and increasing the voltage until breakdown occurs across the dielectric barrier creating a path for the flow of large discharge currents. The results are affected by the rate at which the applied potential is increased and the incremental increases. Rates between 20 V/s and 500 V/s and voltage increments between 10 V and 500 V have been studied. Larger rates cause a premature breakdown compared to a slower ramping speed. This may be due to a kind of conditioning of the sample; the stress of the high voltage is easier to handle if taken in small increases.

(1:42) D1.00002: Orientation Studies of Recrystallized Vanadium Dioxide

Felipe Rivera , Laurel Burk , Robert Davis , Richard Vanfleet – Crystalline films and isolated vanadium dioxide particles (up to 700nm in diameter) were obtained through thermal annealing of amorphous vanadium dioxide thin films on silicon dioxide. Vanadium dioxide undergoes a metal to insulator transition changing from a monoclinic to tetragonal phase near 66 °C. Orientation Imaging Microscopy (OIM) was used to study the phase and orientation of the crystals formed, as well as to differentiate from different vanadium oxide crystal structures. Kikuchi patterns for the tetragonal phase of vanadium dioxide were used for indexing as the Kikuchi patterns for the monoclinic phase are indistinguishable, by OIM, from those of the tetragonal phase. There is a preferred orientation for the growth of these crystals with the c axis in the plane of the specimen.

(1:54) D1.00003: Characterization of Crystallization of Silicon on Alumina

Brady Cox – My research at Brigham Young University this summer focused on studying the crystallization of silicon on alumina (Al_2O_3). I deposited amorphous silicon (α-Si) layers of two thicknesses onto various substrates in order to study how the silicon would crystallize at various temperatures and annealing times. The preliminary results indicate that α-Si does not crystallize at temperatures below 630°C when annealed for an hour on these substrates, but does crystallize at temperatures above 700°C when annealed for the same amount of time. There appear to be no noticeable differences in crystallization between substrates. At the temperatures at which crystallinity was observed, there appears to be no preferred orientation for crystal formation. Further research will focus on determining the lowest temperature(s) at which crystallization begins and studying the early stages of crystal formation at these temperatures.

(2:06) D1.00004: Characterization of GeSbTe Thin Films for Phase-Change Applications

C.D. Grijalva , C.E. Inglefield , T. Herring , Heng Li , P.C. Taylor – Thin films of the alloy GeSbTe are of interest because of current and potential applications in rewritable optical media and reconfigurable electronics. These applications stem from the fact that reflectivity and electrical conductivity are very different in the amorphous and crystalline phases of GeSbTe**,** and rapid switching between these phases is possible**.** We have grown amorphous GeSbTe using RF sputtering on quartz substrates, and used laser-induced heating to switch regions of the film from amorphous to crystalline phases. Previously, atomic force microscopy (AFM) showed that, during this transition, a substantial amount of ablation (several hundred nanometers) of the film occurred. The laser treatment has been revised to reduce the film ablation to the point that it is nearly undetectable by AFM. In addition, the AFM scans of films did not show any ordered structure on the scale we were able to resolve. Future work with these films includes looking at direct measurements of electrical conductivity on a similar scale.

(2:18) D1.00005: Morphological study on dot-chains using molecular beam epitaxy and *in-situ* scanning tunneling microscopy

Haeyeon Yang , Dongjun Kim , Edward Everett , Richard Wilson – We report scanning tunneling microscopy (STM) study on nano dots with a linear alignment. Strained but flat InGaAs epilayers were grown on nominal (001) surfaces of GaAs substrate by molecular beam epitaxy (MBE) at low temperature below 400 ° C. Real-time reflection high energy electron diffraction observations suggest that the strained surfaces are crystalline during the deposition process. *In-situ* scanning tunneling microscope (STM) shows that the strained surfaces are atomically flat but the surface reconstructions are not uniform, mixed with various structures. Upon heating the strained layers above 450 ° C under arsenic pressure, the strained layers undergo roughening transition, resulting in nanodots. The nano dots were formed very closely along a line to form dot-chains during the annealing process. The alignment

lines are mostly along the [1-10] azimuthal direction and some within 35 degrees off the [1-10] azimuthal direction. Furthermore, the size and shape of dots depend on the annealing temperature and strain amount. Effect of strain amount and the annealing temperature on the morphology of dots will be discussed.

(2:30) D1.00006: Linear alignment of InGaAs quantum dots on nominal GaAs(001) surfaces

Dong Jun Kim , Addison Everett , Haeyeon Yang – We report linear alignment of quantum dots (QDs) by direct deposition on smooth surfaces. A single deposition of InGaAs with 37% indium was carried out on a smooth GaAs(001) surface using molecular beam epitaxy (MBE) after a 1μm thick GaAs buffer, whichwas grown at 580° to get a flat surface. The substrate was then cooled down to the InGaAs growth temperature, 500°C. *In-situ* scanning tunneling microscopy (STM) confirmed that the buffer surface was smooth with well ordered 2x4 reconstruction. STM images of the dots show that they are aligned along a terrace edge line as shown while these dots are aligned along the dimer row direction but not along a step edge. The lines in the contour plot indicate the terrace edges and separate terraces with height difference of one monolayer. The effect of growth parameters on linear alignment of self-assembled quantum dots will be discussed.

(2:42) D1.00007: Variation and effects of As_4 flux on morphology of InGaAs quantum dots

E. Addison Everett , Dong Jun Kim , Haeyeon Yang – We present a comprehensive *in-situ* scanning tunneling microscopy (STM) study of InGaAs quantum dots (QDs) on GaAs (001) substrates as a function of arsenic flux using molecular beam epitaxy (MBE). With all other MBE growth parameters fixed, changes in arsenic flux result in changes in the morphology of InGaAs QDs and the critical thickness to form 3D islands. Under arsenic-rich conditions, islands with flat tops are formed while reduced arsenic flux results in formation of islands with rounded tops. Decreasing numbers of InGaAs QDs result from increasing arsenic flux. Reflection high energy electron diffraction patterns taken before InGaAs deposition show that the surface reconstruction changes from a 2x4 to c4x4 with an increase of arsenic flux. STM imaging shows no dots with high As_4 flux, low density of dots with medium As_4 flux, and high density of dots with low As_4 flux, with a deposition amount of 7ML for all samples studied. Effects of arsenic flux on the changes in surface reconstruction surface morphology and density of QDs, and the critical thickness to form the self-assembled QDs will be discussed.

(2:54) D1.00008: Structural Characterization of Nanopolar Domains in PZN-PT

Vayee Vue , Branton Campbell – $Pb(Zn_{1/2}Nb_{2/3})O3$-PbTiO3 (abbreviated as PZN-PT) is of currently of great interest because of its potential as a ferroelectric-relaxor material and because it has the highest known piezoelectric constant. Piezoelectricity is the ability of a crystalline material to generate an electric potential difference when an external stress is applied, or conversely, to generate a physical strain (i.e. stretch or compress) when an external electric field is applied. The physical mechanism that facilitates the special properties of PZN-PT is not well understood. The existence of local structural distortions called nanopolar domains (NPDs) have been suggested as a likely mechanism. We present three-dimensional computer-generated defect models that embody all of the structural freedom an NPD is likely to possess. Individual defect models are evaluated by simulating the x-ray diffuse scattering distribution that results and comparing against experimental data collected at the Advanced Photon Source at Argonne National Laboratory. The DISCUS software package is used to generate the defect models and simulated diffuse scattering patterns, while Crystal Maker is used to visualize the results.

Session D2: Bio-related Physics

Eccles Conference Center - Room 205/207
Friday, October 6, 2006 1:30PM - 3:06PM
Chair: Jean-Francois Van Huele, Brigham Young University
SPS Student Introduction: Kathryn Chapman

(1:30) D2.00001: Developing Serial Diffraction and Microdroplet Beams for Protein Structure Determination

Invited Speaker: R.B. Doak

The first protein structure to be measured was that of myoglobin, in 1958 by John Kendrew, who then remarked "Perhaps the most remarkable features of the molecule are its complexity and lack of symmetry." Indeed, it is this complexity that allows a protein to distinguish a specific molecular species from the thousands with which it might interact. Accordingly, protein structure can offer great insight into protein function but is very challenging to measure. As "lensless imaging" techniques are developed to extract real space structural information from nonperiodic diffraction measurements, serial diffraction of both electrons and x-rays become viable candidates for high-throughput measurement of protein structure. Both probe species require a vacuum environment and hence a means of injecting proteins from solution into vacuum while maintaining the protein in a hydrated form (water soluble proteins) or micellular form (membrane proteins) at all times. Microdroplet beams of the form proposed by Rayleigh in the 1880's offer the ideal tool. This talk will deliver a brief overview of protein structure, discuss the inversion of serial diffraction measurements by "phase retrieval," and then present the requirements, challenges, and various experimental schemes currently directed towards protein structure determination by use of microdroplet beams.

In collaboration with U. Weierstall, D. Starodub, K. Schmidt, P. Fromme, and J.C.H. Spence, Arizona State University.]

(2:06) D2.00002: Fabrication, Cleaning, and Filtering of Microscopic Droplet Beam Nozzles

J. Warner , M. Hunter , U. Weierstall , J.C.H. Spence , R.B. Doak – Structure determination of proteins is a subject of intense current interest. Most relevant is a protein's native conformation, which generally requires it be immersed in water (if water-soluble) or a lipid jacket (if a membrane protein). Emerging schemes of serial protein diffraction propose to embed proteins in microscopic water droplets (membrane proteins encased in a detergent micelle) and pass these in vacuum through an x-ray or electron beam. Droplet diameters of <2 μm and <200 nm are dictated by the respective probe penetration depths. Rayleigh nozzles of <1 μm and <100 nm can deliver such droplets, but clogging becomes a major hurdle at nozzle diameters below even 10 μm. This talk will present an extensive study of the cleaning, filtering, and operation of 4 μm diameter nozzles with intent to minimize clogging. Borosilicate and fused silica nozzles were investigated in both commercial and self-fabricated forms. Equipment was developed to flush the nozzles from both the tip and distal ends. A variety of solvents and detergents were tested, with and without sonication and both before and after the nozzle tip was formed. Flame burnishing was employed to smooth and clean the nozzles. *In situ* formation of silicate filter frits was investigated. Still, only about 30% of the 4 μm nozzles would run without clogging. An alternative to solid convergent nozzles will be described.

(2:18) D2.00003: Breathing interplay effects during proton radiation therapy and development of repainting solutions

Daniel Robertson , Joao Seco , Alexei Trofimov , Harald Paganetti – The movement from passive scattering to active spot scanning in proton radiation therapy introduces the problem of interplay effects when elements of beam motion have a similar time scale to periodic tumor motion, as in a lung tumor. This can lead to significant deviations from the planned radiation dose. Although the repetition of a field over many treatment sessions tends to average out these inhomogeneities, the usual 30 fractions may still leave sizeable errors. These errors are characterized via computer simulation, and field 'repainting' methods are developed to reduce them through increased dose averaging.

(2:30) D2.00004: Lead Levels in Utah Eagles

Michelle Arnold – Lead is a health hazard to most animals, causing adverse effects to the nervous and reproductive systems if in sufficient quantity. Found in most fishing jigs and sinkers, as well as some ammunition used in hunting, this metal can poison wildlife such as eagles. Eagles are raptors, or predatory birds, and their lead exposure would most likely comes from their food – a fish which has swallowed a sinker or lead shot in carrion (dead animal matter). As part of an ongoing project to investigate the environment lead levels in Utah, the bone lead levels in the wing bones of eagles have been measured for eagle carcasses found throughout Utah. The noninvasive technique of x-ray fluorescence was used, consisting of a Cd-109 radioactive source to activate lead atoms and a HPGe detector with digital electronics to collect the gamma spectra. Preliminary results for the eagles measured to date will be presented.

(2:42) D2.00005: Modeling Wave Propagation in Cells and Tissues at the Microscopic Level

Timothy Doyle , Keith Warnick – Several proposed medical therapies and diagnostic methods are

based on the interaction of ultrasonic or electromagnetic waves with cells and tissues at the microscopic level. To better understand these interactions, models are being developed to simulate wave propagation in tissues at the cellular level by incorporating a first-order approximation for the cell structure and multiple scattering between cells. The cells are modeled with a concentric spherical shell-core structure embedded in a medium, with the core, shell, and medium representing the nucleus, cytoplasm, and extracellular matrix respectively. Using vector multipole expansions and boundary conditions, scattering solutions are derived for a single cell with varying properties for each of the cell components. Multiple scattering between cells is simulated using addition theorems to translate the multipole fields from cell to cell and an iterative process to refine the scattering solutions. Results from ultrasonic scattering simulations are presented, including single-cell spectra and wave field images for up to several hundred cells.

(2:54) D2.00006: Energy Computation for nanopore DNA sequencing with an AFM

Shahid Qamar – We are working on a technique to sequence the DNA with an atomic force microscope. Motivated by the experiment, we used an efficient technique to compute free energies of a DNA rotaxne molecule composed of a single strand DNA and a cyclodextrin molecule. Quantitative free energy computation involves milestoning technique with Arrhenius rate equation. The algorithm used computes the time scales of complex processes following the predetermined milestones along a reaction coordinate. A Markovian hopping mechanism was used. We performed the large scale molecular dynamics simulations at micro second level to compute the rare event kinetics which involves large scale distributed computational resources. We performed the molecular dynamics simulations for a DNA rotaxane in the absence of external force to compute the free energy differences among them. All the simulations were performed in aqueous solvent. The theoretical estimation of free energies qualitatively agrees with the experimental data obtained for nano pore DNA sequencing with an atomic force microscope. Initial results show the thermal fluctuations are dominant and the free energy differences between purine and pyrimidine is of the order of $1K_BT$ so the modification of DNA rotaxane is required to suppress the thermal fluctuations.

Session D3: Plasmas and Fusion

Eccles Conference Center - Room 201/203
Friday, October 6, 2006 1:30PM - 3:18PM
Chair: Ross Spencer, Brigham Young University

(1:30) D3.00001: Collisional Braginskii closure vs. the integral closure and closing the fluid equations

J.-Y. Ji , E.D. Held – Recent calculation of the exact linearized Coulomb collision operators and the general moment equations[1] are introduced. As an application, higher order terms for the collisional heat flux closure are derived and the limitation of the collisional Braginskii closure is evaluated quantitatively. For plasmas with general collisionality, the integral heat flux closure based on the pitch-angle scattering operator[2] is introduced and its physical meaning is discussed in comparison with the Braginskii closure. Improvements to the derivation of general closures with a more rigorous treatment of the collision operator and a general scheme for closing the fluid equations are presented.
[1] J.-Y. Ji and E. D. Held, Phys. Plasmas, to be published (2006).
[2] E. D. Held *et al.*, Phys. Plasmas **8**, 1171 (2001).

(1:42) D3.00002: General parallel closures for tokamak plasmas

M. Sharma , J.-Y. Ji , E.D. Held – Analytical and numerical work is done to understand controlled magnetic fusion experiments such as tokamaks, a doughnut-shaped magnetic confinement device that may form the basis of future fusion reactors. In such systems plasma can be described in terms of transport equations obtained from the kinetic equation. We close the density, momentum and energy conservation equations by solving the drift kinetic equation and taking closure moments. A Chapman-Enskog-like approach is adopted where the distribution function is written as the sum of a dynamic Maxwellian and a kinetic distortion, F, expanded in Legendre polynomials $P_l(v_\parallel/v)$. For an accurate treatment of collisional effects, a moment approach is applied to the full, albeit linearized Coulomb collision operator. This approach leads to denumerable infinity of equations describing the system. Truncation at some suitable order permits a derivation of neoclassical closures for the parallel conductive heat fluxes and stresses. The parallel gradient operator, acting on F as well as $v_\parallel/v$, is inverted via the Legendre-polynomial expansion and subsequent diagonalization of the differential equation system for the expansion coefficients is done. This approach allows examination of the closures in all collisionality regimes and thus aids in understanding the complex behavior of confined tokamak plasmas.

(1:54) D3.00003: Implementation and Analysis of 4^{th} Order CWENO Reconstruction for use in Relativisitic MHD Simulations

Nicholas Nelson , David Neilsen – Relativistic magneto-hydrodynamics (RMHD) is used to model astrophysical systems with magnetic fields. Numerical simulations in RMHD require high accuracy to efficiently resolve the complex features expected in the solutions. We discuss an implementation of a central 4th order CWENO method for RMHD. Preliminary results of standard test problems, including comparisons with an established CENO scheme, will be presented and discussed.

(2:06) D3.00004: Non-local plasma heat flow in a perturbed magnetic field

John James , Eric Held – In this work, we review the derivation and implementation of a non-local closure[1] for the field-aligned heat flow in the plasma fluid temperature equation. We apply the closure to a plasma embedded in a sheared slab magnetic field configuration with a single-helicity perturbation and compare derived quantities such as effective radial thermal diffusivity and on-axis plasma temperature with those obtained using a flux-limiting and a local diffusive form for the closure. A novel algorithm for rapid approximation of the heat-flow integrals involved in calculating the non-local closure is presented along with results from validity and convergence tests.
[1] E. D. Held, J. D. Callen and C. C. Hegna, Phys. Plasmas 10, 3933 (2003).

(2:18) D3.00005: Effects of Generalized Ion Stress on Plasma Sound Waves

Michael Addae-Kagyah , Eric Held – Details of two key effects of the generalized parallel ion stress tensor ($\Pi_{||}$) on magnetized plasmas, namely sound wave damping and viscous heating, are presented. Kinetic-based derivation of $\Pi_{||}$, employing an expansion of the particle distribution function, forms the theoretical basis of this study. The goal of this research is to incorporate kinetic physics into the physical models of high-temperature plasmas. Here, a hybrid fluid/kinetic model is applied to the simulation of plasma systems, via the use of the generalized stress closure in the closing of fluid equations. The NIMROD code is used to run the simulations designed to highlight the finite physical effects of the generalized $\Pi_{||}$. Runs involve scans of plasma parameters that correspond to various degrees of plasma collisionality. Analogous simulations, involving the local form of $\Pi_{||}$, are also run for comparison. Diagnostics of the parallel viscosity, damping rates, and energies are made. It is concluded that the generalized $\Pi_{||}$ and the local $\Pi_{||}$models produce similar results at high collisionality, whilst the formerpredicts more realistic values at low collisionality.

(2:30) D3.00006: Construction of a Low-energy Single-wire Z-pinch Apparatus for Metal-catalyzed Fusion Studies

Shannon Walch , Steven Jones , John Ellsworth – Numerous beam and foil experiments have been undertaken in an effort to explore fusion enhanced by condensed matter and have produced substantial evidence for the catalyzing effect of metals and the variation in effectiveness of different types of metal. A group at Brigham Young University studying low energy nuclear reactions is currently building a low-energy single-wire z-pinch apparatus to test it as a tool for producing such reactions. If useful, it will expedite our studying the relationships between the type of metal used and the number of emitted particles, and it will assist in the development of a theory for this type of reaction, as no current theory can predict the outcomes of these experiments.

(2:42) D3.00007: Hollow Plasma Instability: Theory vs. Experiment

Melissa Powell , Grant Mason , Ross Spencer – A Malmberg-Penning trap is a cylindrical apparatus which confines non-neutral plasma (electrons only) with an axial magnetic field and negative electric potentials on both ends. It is a simple system for studying basic plasma behavior, so simple that theory and experiment ought to agree. Theory predicts that a hollow plasma density profile is unstable, and experiments agree. However, the experimental growth rate of the instability is much larger than the theoretical growth rate, by a factor of around 2-4. We are collaborating with Travis Mitchell's experimental research group at the University of Delaware to find the cause for this discrepancy by recreating their Malmberg-Penning trap in our computer simulation. The growth rates of our simulation test cases have remained roughly half that of Mitchell's experiments. We will report the results of investigating several possible causes for this discrepancy, including asymmetry, resistive connections to confining rings, a non-Maxwellian particle distribution function, the initial perturbation, and the polarization drift.

(2:54) D3.00008: Evidence of New Plasma Equilibrium State Sought

William Edwards , Eric Held , Ajay Singh , Jeremy Bishop – A recently reported plasma equilibrium state, derived by minimizing the total system energy without imposing the quasi neutrality condition [1], offers a new possibility for designing a magnetic confinement device for thermonuclear fusion. Utah State University has acquired a small tokamak from the University of Saskatchewan in Canada. This machine is being modified in an attempt to experimentally verify the existence of the state and to determine a procedure whereby a gas at room temperature can be heated to thermonuclear fusion temperatures while held in the new state by magnetic and electrostatic fields. Conditions on size of vessel, gas fill pressure, magnetic field magnitudes, and plasma beta are restricted. A fusion device will be compact leading to the possibility of applications such as production of neutron beams for examination of luggage in airports, search for unexploded land mines, cancer diagnosis, activation of thorium for fission energy, etc.

[1] W. F. Edwards and E. D. Held, *Phys. Rev. Lett.* **11**, 255001 (2004)

(3:06) D3.00009: Generalized Stationary States for Fusion Plasmas

E.D. Held , W.F. Edwards , A. Kullberg – The subject of minimum energy states for magnetically confined plasmas dates back to pioneering work by Woltjer[1] and Chandrashekar[2]Åfter decades of work in this area, a novel theory[3] has been developed which includes all of the terms in the energy integral and adjoins local constraint equations that avoid the common assumption of quasineutrality. In this talk, we discuss a complimentary version of this recent theory which replaces the local constraints of plasma fluid and Maxwell's equations with the constraints of globally conserved generalized helicities. Comparison is made between the stationary states predicted by these theories for the problems of cylindrical Z-pinch, Θ-pinch and screw pinch plasmas. Importantly, both theories predict that substantial electrostatic fields due to charge separation play a critical role in confinement. We conclude by discussing the application of the theory in toroidal geometry which is relevant to the problem of confining fusion plasmas in laboratory experiments.

[1] L. Woltjer, *Proc. Natl. Acad. Sci. U.S.A.* **44**, 489 (1958); **44**, 833 (1958); **45**, 769 (1959)
[2] S. Chandrasekhar, *Proc. Natl. Acad. Sci. U.S.A.* **44**, 842 (1958); **42**, 273 (1956)
[3] W. F. Edwards and E. D. Held, *Phys. Rev. Lett.,* **11**, 255001 (2004)

Session D4: General Physics and Physics Education

Eccles Conference Center - Room 305
Friday, October 6, 2006 1:30PM - 3:18PM
Chair: Brian Pyper, Brigham Young University-Idaho

(1:30) D4.00001: Quantum-mechanical time evolution and uniform forces

Gary Bowman – I consider the time evolution of an arbitrary initial quantum state subject to a spatially uniform but arbitrarily time-dependent classical force. Using the tools of Bohmian mechanics, I show that the state evolves as a free particle state, plus an overall motion arising from the classical force.

(1:42) D4.00002: Searching for photon rest-mass with ion interferometry

Dan Christensen , Brian Neyenhuis , Ross Spencer , Dallin Durfee – We will discuss a proposed scheme to search for a non-zero photon rest mass. This scheme could be more than 100 times more sensitive than previous experiments. The experiment would use an ion interferometer to search for variations in Coulombs inverse-square law predicted by the Proca equation. Analytical and numerical computations will be presented.

(1:54) D4.00003: Experiences Teaching Inquiry-Based Physics to Prospective Elementary School Teachers

Bill Tiernan – I will discuss my experience in teaching a laboratory-based introduction to physics intended for students in the elementary teacher education program at Mesa State College. This course was taught for three years and used the textbook and curriculum "Physics by Inquiry" developed by the Physics Education Group at the University of Washington. In this class students spend most of their time working on exercises and doing experiments, while the teacher circulates and engages students in discussions of their work. In addition to giving an overview of the curriculum I will talk about some of the successes, pitfalls, and difficulties in teaching such a course.

(2:06) D4.00004: Why are you in Physics, Anyway?

Shem Thompson , Brian Pyper – More students leave the major of physics for non-physics majors than visa versa. We surveyed a number of students to pin point their initial reasons to major in physics and their reasons for later leaving physics as a major. Our survey was patterned after Elaine Seymour's research in her book "Talking about Leaving;" her research addresses the issue of attrition in Science, Mathematics, and Engineering majors. The results of our surveys show that the biggest concern physics majors have towards majoring in physics is the fast pace and overwhelming nature of the curriculum. Even students who left a non-physics major to peruse a major in physics reported the Physics curriculum to be overwhelming, a concern they did not have towards their previous major. These same students press on toward their new major in physics inspired by career goals/ opportunities. The influence of career goals/opportunities made possible by majoring in physics appears key in attracting students who would be good at physics but are not initially attracted to the field.

(2:18) D4.00005: Threatened by Gender?

Candice Humpherys , Brian Pyper – A good deal of research has been done on the issue of stereotype threat.[1,2] This research proposes that if a person identifies with a group of people that is negatively stereotyped for performance, then they will not perform as well as someone from the same group of people who is not made aware of the negative stereotype. The research we conducted investigates the legitimacy of stereotype threat based on gender in the area of science in the BYU-Idaho student population. Our results have significance in the current national debate about the lack of women pursuing careers in scientific disciplines. [1]Quinn, Diane M.; Spencer, Steven J.. (2001). The Interference of Stereotype Threat With Women's Generation of Mathematical Problem-Solving Strategies. *Journal of Social Issues.* 57(1):55-71. [2]Schmader, Tony, & Johns, Michael. (2003). Converging Evidence That Stereotype Threat Reduces Working Memory Capacity. *Journal of Personality and Social Psychology.* 85(3):440-452.

(2:30) D4.00006: Does Size Matter? Searching for Rhyme or Reason in Course-End Student Surveys in a Large, Eclectic Physics Department

David Peak – Over the past eight years, surveys of student opinion have been collected (near term-end) in all courses at Utah State University using the same survey instrument. The instrument consists of 25 questions, each of which can be responded to by choosing an integer ranking between 1 ("very poor") and 6 ("excellent"). The University reports a statistical summary of all surveys each term in which all responses are treated equally irrespective of class size (a factor University administrators have asserted is negligible). Discussions of survey content at USU usually focus solely on two items: "rate the course" and "rate the instructor." To some extent faculty tenure, promotion, and salary are based on these two aggregated data. Because of their possible impact on faculty careers, I have examined all responses in all surveys collected over the years in my department. Typical of social data, these results exhibit substantial variability and are highly non-normal. Appropriately treated, however, they reveal a significant class size dependence on the two "rate the..." global items. This fact harbors potentially important policy considerations for departments (like mine) that have a broad range of class enrollments.

(2:42) D4.00007: A Lecture Hall Sized Color Mixing Apparatus

James Coburn – A new apparatus built to demonstrate color mixing by addition in a large lecture hall will be presented. Details will be given on development, design, construction and presentation.

(2:54) D4.00008: Einstein's Meanders

Bradley Carroll – Everyone is familiar with the sinuous meandering of rivers. However, few people recognize Einstein's seminal contribution to our understanding of the origin and evolution of a river's winding channel. This talk will review Einstein's treatment of the fluid dynamics of river meanders. Its simplicity and elegance illustrates his belief that "the whole of science is nothing more than a refinement of everyday thinking."

(3:06)D4.00009: Twisting Relativity Part II: Gravity Behaving Badly

Jerry W. Jensen – We take a second highly speculative look at relativity, rejecting special attributes by varying the medium of space as a function of mass. This time we challenge the veracity Newtonian laws of motion, as well as the time dilation property of special relativity. Space near mass is assigned two important properties: Impedance to motion and an opposing elastic field strength. Both attributes are functions of mass and motion relative to the local mass distribution. These properties provide testable predictions that contrast greatly with the behavior predicted by both the second law of relativity and Newtons second law of motion. A quick perusal of the solar system reveals a cornucopia of stunning observables that are consistent with this abstraction.

Session E1: Physics in the Four Corners Region II

Eccles Conference Center - Room 216
Friday, October 6, 2006 3:45PM - 5:33PM
Chair: Bill Fairbank, Colorado State University
SPS Student Introductions: Cade Perkins, Jan Marie Andersen, Devin Barker

(3:45) E1.00001: Imaging coherent electron flow in a two-dimensional electron gas
Invited Speaker: Brian LeRoy

Images of electron flow through a two-dimensional electron gas are obtained at liquid He temperatures using scanning probe microscopy. Near a quantum point contact (QPC), the images show angular lobe patterns characteristic of the wavefunctions in the QPC. At distances greater than one micron from the QPC, narrow branches of electron flow are observed due to the cumulative effect of small angle scattering. All of the images are decorated by interference fringes spaced by half the Fermi wavelength demonstrating that the flow is coherent. To determine the origin of the interference fringes, an imaging interferometer is created by adding a circular reflecting gate. The strength and position of the interference fringes can then be controlled by the voltage on this reflecting gate. Using the interferometer, we show that the interference fringes are due to backscattering to the QPC. Both experiments and theory demonstrate that the interference signal is robust against thermal averaging.

(4:21) E1.00002: Creating Cold Molecules
Invited Speaker: Heather Lewandowski

The techniques of laser cooling and trapping have transformed atomic physics. The ease of obtaining ultracold atomic samples with these methods has led to new experimentally realizable quantum systems, including the dilute gas Bose-Einstein condensate and the degenerate Fermi gas. After several decades of rapid growth in the field of atom cooling and trapping, the obvious next step is to extend these studies to cold molecules. Molecules have a rich internal energy structure, creating new research opportunities in quantum chemistry, novel collision studies, and collective quantum effects. Cold molecular packets are produced by supersonic expansion coupled with Stark deceleration. First the molecules undergo the expansion process, which cools both the external and internal degrees of freedom. The resulting molecular beam is then slowed to rest by the method of Stark deceleration. Stark deceleration uses the molecules' interactions with inhomogenous electric fields to decelerate the beam. The molecules are then trapped electrostatically, where their collisions can be studied.

(4:57) E1.00003: High Pressure Physics: Thinking Outside the Box
Invited Speaker: Hans D. Hochheimer

I will present examples where thinking outside the box has led to unexpected developments, economic success, and new understanding of the underlying physics. As example of economic success I will present the development of a multipass Brillouin interferometer, which has revolutionized solid state Brillouin scattering experiments. Scientific examples discussed will be alkali cyanides and Chromium alloys.

Session F1: Poster Session

Eccles Conference Center - Third Floor Hallway
Friday, October 6, 2006 5:30PM - 6:30PM
Chair: David Peak, Utah State University

F1.00001: Comparison of Satellite and Ground-Based Data on Polar Mesospheric Clouds

Jodie Tvedtnes , Michael Taylor , Matthew DeLand , Mark Zalcik – Data from the Solar Backscatter Ultraviolet (SBUV) instruments on the NOAA polar orbit satellites have been analyzed to determine the presence of Polar Mesospheric Clouds (PMCs) over the North American continent for five consecutive years from 2001 through 2005. PMCs are ice clouds that form near the mesopause (80-85 km) during summer months at high latitudes. From the ground, these clouds can be seen during twilight hours as Noctilucent or "night shinning" Clouds (NLC) and their occurrence has been growing over the last several decades prompting speculation concerning their role in climate change. For this poster we compare reports of displays seen from the ground over the North American continent primarily by observers participating in the Canadian noctilucent cloud observing network CAN AM with the SBUV satellite data. Our primary goal is to investigate the occurrence and spatial extent of the clouds, as well as to search for unusual low latitude events (<50 deg) that have occasionally been seen as far south as Logan, Utah.

F1.00002: Seasonal Investigation of Variance in Short Period Mesospheric Wave Structure at Low Latitudes

Hema Karnam , Mike Taylor , Jake Gunther – As a part of the Maui-MALT program, the Utah State University Mesospheric Temperature Mapper (MTM) has operated continuously at Maui-Hawaii since November 2001. Over 1000 nights of high quality data on Mesospheric temperatures using the near infra red OH and O_2 emission layers (centered at 87 and 94 km respectively) have been obtained over the past four years. In this study, we have analyzed data from 2003 (295 nights) to perform an initial investigation of the variance in OH and O_2 signal in the frequency band corresponding to short period (12 min- 1 hour) . This was done by spectrally filtering the data into selected bands (approximately 1 hour wide). The data have been used to study variability in wave content on a night-to-night as well as a seasonal basis. Short period waves were present throughout the year and indicate no obvious summer to winter difference in wave power. On sporadic nights throughout the year, both OH and O_2 show remarkable enhancements of wave power (factor of 10). Here, we present the results of this initial study.

F1.00003: Investigating the horizontal characteristics of the short-period gravity waves over Bear Lake Observatory, Utah

Deepak Simkhada , Michael Taylor , Robert Stockwell – The horizontal characteristics of short-period gravity waves were observed in the OH airglow layer at $\sim$ 87 km during a one year period in 2002 from Bear Lake Observatory, Utah (41.90 N, 11.40 W). These waves typically have short periods (6-15 min) with short horizontal wavelengths (8-35 km) and horizontal phase speeds of (20-65 m/s). All the wave events fall into two groups, bands and ripples. The band structures appear as a train of wave fronts with a horizontal wavelength larger than 15 km and the ripples were small-scale structures with a horizontal wavelength less than 15 km. In summer, most waves propagated towards the N- NE, whereas, in winter, wave propagation directions were towards the NW and SW. The observation suggests that these waves were propagated from the lower atmosphere and filtered in the middle atmosphere by the mean background winds.

F1.00004: A Niching Genetic Algorithm For Milne-Eddington Spectral Line Inversions

Brian Harker , K. Balasubramaniam , Jan Sojka – Stokes profile inversions form a basis for "measuring" solar magnetic fields. The High Altitude Observatory (HAO) Milne-Eddington (M-E) spectral line inversions have traditionally been used as initializations to more sophisticated inversion procedures. One such code uses a genetic-algorithm initialization to search the parameter space on a more global scale, in an effort to obtain a good starting guess for a more traditional hill-climbing (e.g. Levenberg-Marquardt) algorithm. A serious drawback to the type of genetic algorithm used is that it has been shown to perform poorly on high-dimensional spaces with multiple optima. A single-component M-E model atmosphere is typically described by about 7 free parameters, indicating a fairly high parameter space dimensionality. Two-component models increase the ability to fit frequently-observed asymmetric spectral lines, at the price of nearly doubling the dimension of the parameter space. Furthermore, spectral lines for large magnetic field strengths and large inclinations are very similar to profiles for weaker field strengths and small inclinations, indicating the potential presence of multiple optima that correspond to very different physical conditions. This poster presents an initial investigation into alleviating these difficulties by incorporating a more sophisticated evolutionary strategy into the SGA, and parallelizing over multiple processors.

F1.00005: Polar Crater Deposits as a Probe for Ancient Climate Change on Mars

John Armstrong – Dynamical studies of the Martian orbit suggest a planet that has undergone extreme orbital change. How has this affected the planet's climate? Is there a record of this orbit-induced climate

change written in the geology that is expressed on the surface? If so, such a record would provide insight into Mars' climate history, and shed light on the types of habitats for life that may have existed in the past. We are exploring how the current seasonal polar caps interact with polar craters in an effort to identify modification that can be linked to the proximity of the polar cap. Ice deposits within the craters are evident in both thermal spectra and imagery from Mars orbiters. We have linked these ice deposits to morphological deposits that can be identified in other craters that are further from the pole. These deposits may act as a probe of the variations suggested by orbital calculations, as well as provide an indicator of the extent of the sub-surface ice table. We will present preliminary results from a sample of northern craters, and explain how this can be extended to southern craters, and possibly mid-latitude craters, in an effort to understand more fully the martian climate through time.

F1.00006: Green Thumbs for the Red Planet

Jacque Jackson , David Allred , Niki Brimhall – In the famous book, The Case for Mars, Robert Zubrin discusses how resources readily available on Mars could easily be used to construct a greenhouse. This project tests his proposition that plants can be grown in Mars-ambient levels of carbon dioxide. Previous tests have shown that it is possible for plants that have been growing under normal conditions can survive for a period of time in Mars-ambient levels of carbon dioxide, but it has not yet been tested exactly how long they can live under such conditions, nor whether they can be planted and grown in such conditions. We also propose an excellent candidate for a Martian greenhouse plant, namely a Bolivian grain called quinoa. Quinoa is efficient because the entire plant's leaves, root, stem, and fruit are edible and nutritious. Also, quinoa is promising because it is a robust plant accustomed to low pressures and cold temperatures. If it proves possible to grow and cultivate plants in Mars-ambient levels of carbon dioxide, future exploration of Mars would be greatly benefited.

F1.00007: Exploring "Freeze Out" on Mars using an Atmospheric Circulation Model

Michael Esquivel – In addition to observational research, computational models like the NASA Ames Mars General Circulation Model (GCM) are used for efficient and often detailed representations of physical quantities. Using this GCM model, I am studying the effects of the distribution and density of frozen carbon-dioxide located at the polar caps. I have paid attention to the effects of the resulting ground temperature, surface pressure, and ground ice through time-based 2D and 3D animations. Also, I have modified the planet's axis between 5 and 50 degrees, changed the pressure by orders of magnitude from zero to two magnitudes, and studied conditions that result to a time frame of nearly 4 billion years ago. Preliminary results show that low pressures with low degrees of tilt have resulting pressures that approach zero, often ending simulations early. The remaining frozen carbon-dioxide remains airborne which could explain the possibility of an atmospheric phenomenon called a "freeze out." This type of atmospheric computational data is often tedious and cumbersome to interface between numerical data and visual format. To counteract this problem, I have built an interface using IDL to interact with raw Mars GCM data. This interface allows researchers to increase the time to study actual science and minimize the time to find and decipher data to a visual format. This interface allows modification of initial variables to allow for cold starts of the Mars GCM model as well as create new maps and view them in an animation sequence to study changes in time.

F1.00008: Generalized Stationary States for Plasmas with Conserved Global Helicities

A. Kullberg , E.D. Held , W.F. Edwards – After decades of work on the subject of minimum energy states for plasmas, a novel theory[1] has been developed which includes all of the terms in the energy integral and adjoins local constraint equations that avoid the common assumption of quasineutrality. In order to verify the predictions of this theory as well as extend it to toroidal geometry, we present complimentary work that constrains the variation of total plasma energy under the assumption of conserved global helicities. The resultant Euler-Lagrange equations take the form of coupled, nonlinear partial differential equations for the magnetic and electric fields, plasma flows and densities and the Lagrangian multipliers associated with conserved global helicities. Assumptions regarding symmetry are then employed to convert the Euler-Lagrange equations to coupled ordinary differential equations which are solved using finite-difference, relaxation techniques. Quantitative comparisons of the solutions from these theories are made for the problems of diamagnetism in slab geometry, which is relevant to space plasma in the Venus ionosphere, and cylindrical screw pinches, which is relevant to the confinement of fusion plasmas in the laboratory. Preliminary work regarding minimum energy states in toroidal geometry is also presented.

[1] W. F. Edwards and E. D. Held, *Phys. Rev. Lett.,* **11**, 255001 (2004)

F1.00009: Experimental Verification of a new Plasma Equilibrium State

Jeremy Bishop , Ajay Singh , Farrell Edwards , Eric Held – It has been shown that a "steady state equilibria of two-species collisionless plasmas have been found for symmetrical systems by varying the total energy subject to Maxwell's equations, momentum moment equations, and adiabatic equations of state, without imposing a quasineutrality condition"[1] We have undertaken the task of experimentally verifying that these equilibria exist. In order to do this we have received delivery of equipment from the University of Saskatchewan, consisting of the the components of the tokamak STOR

– 1M. After restoration to working condition, we will modify the equipment to encourage the formation of the equilibrium state. Additional testing will be used to determine feasibility to applications such as neutron and/or power generation. Currently, we are in final preparation for vacuum testing, after which we will complete restoration of the electrical system including capacitor testing,a new optically isolated control system and installing required diagnostics. This will allow us to have first plasma in December 2006.

[1] W. F. Edwards and E. D. Held, *Phys. Rev. Lett.,* **11**, 255001 (2004)

F1.00010: Phi Meson as Probe for Quark Gluon Phase Transition

Z. Yasin – Vector mesons provides crucial direct signals for characterization of the early times of the quark gluon phase transition predicted at temperature around 150 MeV. Since, Phi Meson is not masked behind other resonances in mass spectra so it provides a nice probe to verify the standard model prediction of chiral symmetry restoration, expected to cause modification of its mass, width and decay channels in the dense hadronic matter. Creation of such a state of matter is main objective of current series of ultra-relativistic heavy ion collision experiments at Brookhaven National Laboratory. Monte Carlo simulations can be used for tracking charge particles through complex detectors. Results from a Monte Carlo Carlo simulation code, developed for verifying the QCD phase transition signals for Phi Meson, will be presented.

F1.00011: The Equation of State of α-Uranium from a First Principles Perspective

Sourav Adak , Boris Kiefer – Uranium occurs in diverse environments, for example as a fuel in nuclear reactors and as a major source for the internal heating of our planet. Therefore the understanding of the electronic structure of uranium is important to develop a unified model for uranium in different bonding environments. Heavy elements at the bottom of the periodic table pose a large challenge to theory due to the often complex interplay of s-, d-, and f-electrons that are difficult to treat self-consistently in density functional theory. Here we adopt the simplest description that neglects spin-orbit coupling and any special treatment of strong electronic correlations. The calculations are based on the projected augmented wave method within the GGA approximation. We find that the equation of state is in good agreement with experiment. This suggests that our simplified electronic structure model of uranium captures most of the physics and may be used to describe bonding of this element in other environments at least to first order.

F1.00012: Roughness Contributions to Thin-Film Reflectance

Elise Martin , Jedediah Johnson , R. Steven Turley – In order to find a factor to account for how surface roughness affects reflection and transmission measurements of thin films, we developed a MATLAB program that computes scattering from a rough surface with arbitrary-good accuracy. S-polarized plane waves are reflected off of a perfectly conducting surface with a certain amount of roughness and normalized with reflection from a perfectly smooth surface. In order to best model the kinds of roughness we anticipate in actual thin films, the surfaces were created with cubic splines where the spacing of the knots was varied to control the spatial frequency. The heights of the knots had a random Gaussian distribution. To make these computations useful for extracting index of refraction data from thin-film reflectance measurements, we have developed efficient approximations of the exact calculations that can be used in data fitting programs. These approximations give the roughness correction as a function of incident angle, root-mean-square roughness, and spatial frequency.

F1.00013: Time-Space analysis on spreading processes in small-world networks

Lin Xue , Zhihuai Zhu , Qi Zhang , Peng Zhang – We used time-domain statistical analysis to study the spreading processes on one-dimensional small-world networks. The relationships between the saturated infection rate and both spatial and temporal parameters of the system were studied. We found that the saturated infection rate increase exponentially with the mean degree and linearly with the ratio of the shorts cuts while it is almost independent of the size of the network when the network is large enough, which could not be observed without considering the spatial structure of the model. The infection probability and the active period also influence the saturated infection rate. The obtained results may provide insights into a prognosis of a spreading process in closed system especially for epidemic control.

F1.00014: Using Linear Delta Expansion for the Solution of the Schrödinger Equation

Luis M. Sandoval , Jorge A. Lopez – In this work, we present a solution to the Schrödinger equation using a method known as Linear Delta Expansion (LDE). The method utilizes different scaling behavior that is found at different distances. In particular, we can identify three ranges of scaling behavior, which can be solved independently. At large distances, we observe an asymptotic behavior that depends only on the form of the potential. The intermediate scale is based also in exponential decay of the wave function. Finally, for short distances, the wave function is sizable. We used this method to solve the quantum anharmonic oscillator, and we obtained good results employing only algebraic equations.

F1.00015: Reconstructing Systems of Nonlinear Differential Equations from Time Series

Keith H. Warnick , Charles R. Tolle – Appropriately modeling a dynamical system by the construc-

tion of differential equations is a vital and common task in computational physics. However, generating an acceptable model of the underlying dynamics may be a complex problem in systems which exhibit high-order or nonlinear behavior. This poster details the reproduction and performance of a trajectory method proposed by Perona et al. for the construction of a system of nonlinear differential equations from time series data. By numerically integrating a given set of basis functions, the method uses an iterative algorithm to fit a polynomial in the chosen basis functions to the time series. By this method, time series data from any sufficiently connected and observable system may potentially be used to numerically approximate the equations which give rise to the system dynamics. The demonstrated generality and effectiveness of this method make it a potentially powerful tool for the study of dynamical systems.

F1.00016: A thermal beam calcium matter-wave interferometer

Jeremiah Birrell , Dan Christensen , Christopher Erickson , Justin Paul , Rebecca Tang , Dallin Durfee – We report on progress toward a calcium-beam atom interferometer. The design uses a novel alignment scheme using precision prisms which will cause first-order Doppler shifts to cancel out to high accuracy. The device will utilize a thermal beam of atoms for simplicity and high signals. The atom waves will be split and recombined using a single-photon transition at a wavelength of 657 nm. We are currently working to improve the linewidth of the 657 nm laser and constructing a 423 nm blue laser to transversely cool the atoms and to detect the output of the interferometer. We are also characterizing a thermal Ca beam using laser absorption and working on precise control of the temperature and flux of the beam.

F1.00017: Study of Adsorption Isotherms Using Micromachined Quartz Crystal Gravimetric Sensors

Jay Mathews , Abhijat Goyal , Srinivas Tadigadapa – Using microfabrication techniques, it is possible to realize gravimetric sensor platforms which can resolve mass down to a few femtograms and are robust enough to operate even in aqueous ambient. In this study, an ultra-sensitive quartz crystal microbalance (QCM) was used to study the self-assembly of thiol-based alkyl molecules on the gold electrode of the QCM and subsequent specific adsorption of protein molecules on top of the grown Self Assembled Monolayers (SAMs). Specifically, isotherms for formation of monolayers of 1-hexadecanethiol were generated, as well as adsorption isotherms for proteins such as human serum albumin (HSA) on the grown monolayers. Such fundamental studies using gravimetric sensor platforms with unprecedented sensitivity are expected to result in better understanding of the biological processes in the human body, better control over the self-assembly process, and possibly in realizing a System on a Chip (SOC) entirely through the self-assembly process.

F1.00018: Velocity measurements of hohlraum-driven beryllium "flyer" plates

T. Tierney , J. Cobble , N. Hoffman , B. Devolder – In indirectly-driven fusion experiments, energy-coupling between a laser-driven cylindrical hohlraum and the fuel-containing ablator material governs the maximum attainable yield. In the case of the National Ignition Facility, a class of capsules uses copper-doped beryllium ablators containing deuterium-tritium fuel to absorb in excess of 100 kJ of soft x-rays and would hypothetically achieve fusion ignition. In these experiments, planar 0.9% copper-doped beryllium slabs are mounted on one axial end of a 1.6-mm diameter, 1.2-mm long cylindrical hohlraum. The hohlraum is driven with $\sim$4 kJ of laser energy to radiation temperatures near 150 eV with a 6-ns drive. Bulk hydrodynamic motion of the slab, induced by radiative drive, is measured using side-on x-ray imaging. The slabs' velocities provide estimates of the time-integrated energy received by the beryllium. We present the experimental design and initial results.

F1.00019: Instrumentation for Measuring Radiation Induced Conductivity of Insulating Materials

Joshua Hodges , J. Corbridge , J.R. Dennison , R.C. Hoffmann , J. Abbott , A. Hunt , R. Spaulding – We report on new instrumentation to measure Radiation Induced Conductivity (RIC). RIC occurs when incident ionizing radiation deposits energy in a material and excites electrons into the conduction band of insulators. Conductivity is determined by measuring the current through the thin film samples in a parallel-plate geometry under a constant applied voltage. RIC is calculated as the difference in the equilibrium sample conductivity under no incident radiation and sample conductivity under an incident flux. An accelerator beam at the Idaho Accelerator Center provides the 2-5 MeV incident flux over a range of 10^{-2} to 10^{+1} rad/sec. Measurements are taken simultaneously from 10 large thin film samples (90 cm^2). Radiation passes through a 4 mm thick stainless steel window that is used to provide a vacuum environment to prevent arcing and contamination. Detail of the instrumentation and preliminary results will be presented.

F1.00020: Measurements of the Radiation Induced Conductivity of Insulating Polymeric Materials for the James Webb Space Telescope

J. Corbridge , J.R. Dennison , J. Hodges , R.C. Hoffmann , J. Abbott , A. Hunt , R. Spaulding – We report on initial measurements of *Radiation Induced Conductivity (RIC)* for twelve thin film polymer materials that are used in the cabling of the James Webb Space Telescope. Results will be used to model possible detrimental arching due to space craft charging effects. RIC occurs when incident ionizing radiation deposits energy in a material and excites electrons into the conduc-

tion band of insulators. RIC is determined using a constant voltage test method as the difference in the equilibrium sample conductivity under no incident radiation and sample conductivity under an incident flux. An accelerator beam at the Idaho Accelerator Center provides the 2-5 MeV incident flux over a range of 10^2 to 10^{+1} rad/sec. Measurements are made for a range of applied voltages and radiation dose rates.

F1.00021: Effects of Fluence and Charge Density for Pulsed, Low-Fluence Measurements of Electron Emission in Highly Insulating Materials

Ryan Hoffmann , J.R. Dennison – Accurate measurements of the electron emission properties of extreme insulators require highly controlled experimental techniques. Due to the poor electron mobility in insulators, charge can accumulate which will affect future incident and secondary electrons; subsequently, the electron yield will evolve. This evolution is the prime difficulty in measuring the electron yield of insulators. Minimizing the charge in the electron probe using a pulsed, low-current electron beam will largely mitigate these effects. However, to accurately measure the insulator secondary and backscattered electron yields, careful control is required of the beam current magnitude and spatial charge density. Methods for accurately determining pulsed electron beam fluence and charge density profiles will be discussed. The effects on the yield, emission spectra and yield decay curves—as dose per unit area is varied—will also be presented.

F1.00022: Dynamics of high frequency magnetization reversal in nanomagnets

Zhihuai Zhu – The magnetization reversal of two-dimensional nanomagnets driven by high frequency magnetic field is investigated by numerically solving the Landau-Lifshitz-Gilbert equation. It is observed that the hysteresis dispersion, i.e. hysteresis area A as a function of f, exhibits the second resonance once the in-plane effective field is nonzero. The dynamics of this resonance shows some chaotic behaviors, and originates from the transition between the steady state with a small precessional oscillation and a metastable state with a large-angle reversal. Over the high f range, the loop area A for a fixed f oscillates with time t and each component of magnetization shows a periodic maximal reversal. The oscillation of A(t) relates to that coexistences of precessional modes alternately appears in the systemic configuration. Finally, large domains and a size effect on A(t) also are exhibited under a strong exchange interaction.

F1.00023: Electrical properties of nanocrystalline ZrO_2 at high-pressure

Anna Trefilova – It is shown, that the materials are received from nanocrystallite zirconium oxide have the different properties from bulk material. The combination of external compression and the contribution of a surface create an opportunity of occurrence of the unusual physical and chemical and electrophysical phenomena. Research of such effects is necessary for development of fundamental bases of creation new materials with special properties. We studied correlation between the sizes of crystallite and resistance ZrO_2 at the pressures 22 - 50 GPa and temperatures 77 - 400 K. The dc resistance measurements were carried out in a diamond anvil cell rounded cone-plane type. We found that the transition pressure of ZrO_2 depends on crystallite size. The smaller crystals, the smaller transition pressure. The reduction of transition pressure was observed to 10 nm. However at 10 nm the transition pressure rises steeply. It is possible to suspect, that the surface effects essentially change ZrO_2 conductivity mechanism at high pressures. We studied relaxation processes in ZrO_2 under the high pressures and the room temperature. The analysis of experimental data has shown that the time function of electric resistance most precisely described by exponential function. It can be seen, that relaxation times depend on pressure and crystallite size.

F1.00024: Electrical resistivity measurements of the chalcogenide spinel, $CuIr_2S_4$, under extreme conditions

Mark Hanni – Electrical resistivity as a function of pressure will be investigated for the thiospinel compound, $CuIr_2S_4$, which exhibits a metal to insulator transition at high pressures. This study will corroborate existing experimental and theoretical work and is the first of its kind to perform high pressure electrical conductivity and insulating phase optical studies in the range of room temperature to liquid nitrogen temperature. In addition, the transport properties of adamantine semiconductors will be studied at high pressure. The resistivity measurements will be made using a pseudo four-wire probing technique, using an AC constant current source, to eliminate thermal noise in the connections, and a nanovoltmeter. The study is currently ongoing and results are still pending. Improvements made to a stepper motor control program and changes to the system used for optical studies will be presented.

F1.00025: Ultrasonic studies of Ti-Zr-Ni Quasicrystals

Truman Wilson , Dennis Agosta , Robert Leisure – Quasicrystalline materials lack the translational periodicity of ordinary crystals, yet are highly ordered. In particular, they have rotational symmetries forbidden for crystals made of repeating unit cells. Much is unknown about the structure and interatomic interactions of these materials. Elastic constants are sensitive to both the local structure and the interatomic potentials. Resonant ultrasound spectroscopy was used to study $Ti_{39.5}Zr_{39.5}Ni_{21}$ quasicrystals. In this technique the vibrational eigenmodes of small parallelepipeds are excited and analyzed to determine elastic constants and ultrasonic loss. The experiments were carried out over the temperature range of 3 – 500 K. The bulk, shear, and Young's moduli, as well as Poisson's ratio were determined. The ultrasonic loss was also studied. The temper-

ature dependence of the elastic constants resembles that of ordinary metals, approaching 0 K with zero slope, and becoming linearly dependent on temperature at higher temperatures. The ultrasonic loss shows a broad peak centered near room temperature, which may be associated with phason flips.

F1.00026: Making an ultrastable diode laser

James Archibald , Matt Washburn , Marshall van Zijll , Christopher Erickson , Brian Neyenhuis , Greg Doermann , Dallin Durfee – We have constructed a 657nm diode laser with excellent stability for use in an atom interferometer. The laser is a grating-stabilized diode laser is locked to a high-finesse cavity using the Pound-Drever-Hall method. We have measured a linewidth of about 1 kHz and are working on several improvements which should further reduce our linewidth.

F1.00027: Study on energetics of self-assembled quantum dot using molecular beam epitaxy and *in-situ* scanning tunneling microscopy

Richard Wilson , Dong Jun Kim , Addison Everett , Haeyeon Yang – A chain of quantum dots were observed to form during an annealing process. Strained but flat InGaAs epilayers were grown on nominal (001) surfaces of GaAs substrate by molecular beam epitaxy (MBE) at low temperature below 400 $^\circ$C. Real-time reflection high energy electron diffraction observations suggest that the strained surfaces are crystalline during deposition processes. *In-situ* scanning tunneling microscope (STM) shows that the strained surfaces are atomically flat and the surface reconstruction are mixed with various structures. Upon heating the STM observed samples above 450 $^\circ$C under arsenic pressure, the strained layers undergo roughening transition, resulting in nanodots. The size and shape of dots depend on the annealing temperature and strain amount. Furthermore, the dots are aligned along straight lines, forming chains of dots.

F1.00028: Quantum Dot Modulators

Brendan Turner , Manish Mehta , Ramesh Laghumavarapu , Diana Huffaker – Mach-zender devices are an ideal modulation source for communication networks at 1.3 μm and 1.55 μm. Superlinear electro-optical effects are a desirable feature in mach-zender modulators since their large second order electro-optical coefficient would give complete signal extinction at a small voltage. Quantum dot devices show promise for such applications in the 1.3 μm band. In this project we performed free-space characterization of stacked InAs quantum dot devices. A crossed polarizer and analyzer combination were used to determine the phase retardation/voltage relation and electro-optical coefficients for said materials. We used different pump wavelengths to analyze their effect on modulation. Further calculations were carried out to determine the theoretical extinction ratio of such devices as part of a mach-zender modulator.

F1.00029: One dimensional array of QDs for a single InGaAs layer deposition on a smooth (001) surface of GaAs substrate

Joseph Abel , Dong Jun Kim , Addison Everett , Haeyeon Yang – The formations of quantum dot arrays during the growth of InGaAs/GaAs were reported using multiple layers or high index on the GaAs substrates. The lateral orderings are formed on the capping layer with reduced lateral strain. The other types of arrays were shown by surface diffusion from the substrates at a corrugated surface, such as the edge of terrace. In this study, we directly suggest one-dimensional array on a flat surface of single layer deposition. The sample growth process was performed by molecular beam epitaxy, which connects to a scanning microscope. A 1μm thickness buffer was grown at 580 $^\circ$C to get a flat surface. The surface condition was checked by RHEED. $In_{0.4}Ga_{0.6}As$ on GaAs (001) substrate was grown at 500 $^\circ$C with higher arsenic flux than GaAs substrate structure transition amount. The topographic properties of the grown samples were characterized by in-situ STM. Each growth has different InGaAs thickness, from 7.5ML to 6.1ML. In conclusion, we have proposed the new model of InGaAs dot arrays on the GaAs(001) surfaces. Some assumption will be discussed on more experimental results.

F1.00030: Crystal structures of Th(Cu,Sn) compounds

Farzana Nasreen , Luis M. Sandoval , Karunakar Khotapalli , Alexandre V. Andreev , Heinz Nakotte – Powderized samples of Th(Cu,Sn) with nominal compositions of 1:1:1 and 1:2:2 were studied by neutron diffraction techniques using the NPD diffractometer at the Los Alamos Neutron Science Center. The structural analysis of the diffraction data was done using the Rietveld refinement package GSAS, which was developed at Los Alamos National Laboratory. For ThCuSn, assuming an orthorhombic structure with P21cn space group fits the neutron-diffraction data best. We still observed some unindexed reflection, which could be attributed to thorium dioxide as the second phase. The second sample was thought to be ThCu2Sn2, which crystallizes in the tetragonal P4/nmm phase. A careful analysis of the intensities revealed that not all of the Cu positions for this composition are occupied and that the actual composition of our second sample is closer to 1:1.5:2. A similar observation was reported for the magnetic analog UCu2Sn2.

F1.00031: Production and Examination of Nanocrystalline Copper

Jennifer Albretsen , James Hanna , Qi Zeng , Ian Baker – 325-mesh copper powder was ball milled under various conditions to produce copper samples of different grain sizes. One well-milled sample was annealed at varying temperatures and for different times to promote grain growth. These two procedures provide a range of grain sizes for study. Crystallite size was de-

termined by analyzing x-ray diffraction peak broadening. Continuing research would include equal channel angular extrusion (ECAE) of the samples in an attempt to produce bulk nanocrystalline copper, allowing researchers to more easily determine the mechanical properties of this nanocrystalline metal.

F1.00032: Toward single Ba or Ba^+ detection on a fiberoptic tip

Shon Cook – In progressing toward Ba and Ba^+ single atom tagging in solid Xe, an efficient laser delivery and fluorescence detection system is needed. One method is the use of an optical fiber for delivery of the laser beam and the same or a different fiber for collection of the fluorescence. Various designs and requirements for accomplishing single atom or ion detection are discussed and initial measurements of scattered light in the fiber(s) are presented. Single atom detection is a reasonable expectation.

F1.00033: Temperature Calibration for Sample Heating in Ultrahigh Vacuum

Heidi Wheelwright , T.C. Shen – Precision temperature measurement is a challenge for ultrahigh vacuum sample preparations. Thermocouples and pyrometers can be used to measure the temperature of samples, but these two techniques need calibration. We have made a mathematical model to calibrate the thermocouple readings with the pyrometer readings. This model is based on equations considering the input power and the heat loss by conduction and radiation. The heat conduction constant is determined from pyrometer temperature measurements at various power inputs. Given any input power, this model will return a temperature value that agrees very closely to the thermocouple readings which have been calibrated with the pyrometer.

F1.00034: A Temperature-driven Liquid Xenon Recirculation and Purification System

Julio Cesar Benitez-Medina , Kendy Hall – We have built a liquid xenon recirculation and purification system in order to address the problem of inconsistencies in our Ba^+ fluorescence spectra. In our previous work our liquid xenon purity system did not include recirculation, and the liquid xenon contained ppm of electronegative impurities. By continuous recirculation through a getter purifier, ppb purity is expected. Our recirculation system is driven thermally, by applying heat to the evaporation region, instead of by the pump method used by others. The advantage of thermal driven recirculation is that there are no pressure surges. Therefore, the liquid is calm as it evaporates and condenses. This gives excellent optical quality for Ba^+ spectroscopy in liquid xenon. The goal of this work is to detect fluorescence from single Ba^+ daughter ions in the Enriched Xenon Observatory (EXO) double beta decay experiment.

F1.00035: Phases of Ultra Cold Gases in the Fermi-Bose Hubbard Model

Daniel Schirmer – The experimental realization of a BEC has stimulated the interest in theoretical models of zero-temperature quantum phase transitions. Ultra cold gases confined in optical lattices can demonstrate a wide range of different phases by varying controllable system parameters, such as optical lattice intensity, particle number, spin composition and the inter-atomic interaction. This project aims to unveil phases in a one dimensional system of fermions coupled to a bosonic molecular state, in the limit of an infinite number of lattice sites. This is accomplished by solving the Fermi-Bose Hubbard model using a numerical method developed by G. Vidal [G. Vidal, Phys. Rev. Lett. 91, 147902 (2003)], and implemented into a Mathematica package by J. E. Williams at NIST, which was used extensively in my research. This research focuses on calculating diagrams of the homogeneous system as functions of nearest neighbor hopping energies, onsite fermion chemical potential, onsite fermi-bose coupling strength, and a detuning factor, determining relative boson chemical potential. For most calculations, onsite interactions are not considered. Because ultra cold gases are possible to create, manipulate, and observe, they function as a future test bed for studies in solid-state physics and quantum computation. Theoretical tools such as phase diagrams are especially important to the development of these fields.

F1.00036: Searching for Tertiary Companions to Eclipsing Binary Systems in the LMC

Michael Malmrose , Stacy Palen – We use a new method to search for possible tertiary companions to EB's in the MaCHO database. By binning the light-curve data and averaging the magnitude, we derive an average light curve by linear interpolation. This curve is directly compared to the observed data. The O-C phase is determined by subtracting the phase of a data point from the phase when the average curve has the same magnitude. This is done for both the primary and secondary eclipses. The O-C data are then plotted as a function of time. We use a Lomb periodogram to search the O-C data for high power signatures in a range of frequencies, yielding periods of possible tertiary companions. We phase-fold the O-C data obtained from both red and blue filters. We currently observe the signature sinusoidal variations of a tertiary companion in two systems for both wavelengths. We suspect that these two objects are stellar in nature.

F1.00037: Chemical Patterning by Mechanical Removal of Aqueous Polymers

Katherine Barnett , Jodi Knoebel , Robert C. Davis – We are developing a new method for micro and nanoscale patterning of lipids and proteins on solid surfaces. A layer of polyethylene glycol (PEG) teminated polyallyl amine (PAA) was initially applied to a mica surface. The PEG surface is a low adhesion surface for proteins. Following polymer deposition an Atomic Force

Microscope (AFM) tip was used to remove the polymer layer in desired regions. AFM imaging of the surface after mechanical polymer removal shows squares of exposed MICA surrounded by the PEG surface. The clean mica regions are now available for specific adsorption of lipid or protein layers.

F1.00038: Spectroscopic Ellipsometry And Variable-Angle XPS Scanning

Liz Strein , Amy Grigg , David Allred – The extreme ultraviolet portion of the EM spectrum from 10-100 nm is becoming increasingly important in various technological applications. However, the optical constants in this region are not well known and need further determination. This is done by observing the interaction of EUV light with thin metallic films. It is essential that the composition and thickness of the film are well characterized in order to determine the optical constants. Depth profiling and angle resolved x-ray photoelectron spectroscopy (XPS) are used to characterize the composition of the films. The extent of oxidation at the surface of the films is of particular interest. Current research is focused on determining how spectroscopic ellipsometry and variable-angle XPS scans increase understanding of this oxidation.

F1.00039: Effects of As_4 flux on morphology of InGaAs quantum dots and the critical thickness

N. Lambert , E. Addison Everett , Dong Jun Kim , Haeyeon Yang – We present a comprehensive in-situ scanning tunneling microscopy (STM) study of InGaAs quantum dots (QDs) on GaAs (001) substrates as a function of arsenic flux using molecular beam epitaxy (MBE). At 500°C and with all other MBE growth parameters fixed, changes in arsenic flux result in changes in the morphology of InGaAs QDs. Increasing arsenic flux results in decreasing numbers of InGaAs QDs. Reflection high energy electron diffraction patterns taken before the InGaAs deposition show that the surface reconstruction changes as a function of arsenic flux. The arsenic fluxes were kept the same during the subsequent $In_{.4}Ga_{.6}As$ deposition. After the deposition, the MBE grown samples were cooled down to room temperature by turning the growth stage heater off. The samples were then taken into the STM chamber via ultra-high vacuum port. STM images of InGaAs deposition show no dots with high As4 flux, and very high density of dots with low As4 flux. Effects of arsenic flux on the changes in surface reconstruction surface morphology and density of QDs, and the critical thickness to form the self-assembled QDs will be discussed.

F1.00040: Infrared Imaging of Transient Luminous Events (1 1.5 microns) Over the Mid Western US and Comparison with their Visible Wavelength Signatures

Matt Bailey , Michael J. Taylor , Dominique Pautet , Walter A. Lyons , Steven Cummer – As part of a coordinated campaign conducted from Yucca Ridge, Colorado during summer, 2005, four sensitive imaging systems were fielded by Utah State University to investigate the signatures of transient luminous events (TLE's) over a broad spectral range, extending from the near ultra violet (0.35 microns) to infrared wavelengths (1.5 microns). These measurements were made in conjunction with high speed video and electromagnetic observations providing detailed information of the TLE dynamics and their structures. The USU instruments consisted of two Gen 3 Xybion cameras, one filtered to observe N_2 first positive emissions (665 nm) while the second observed white light emissions. A third intensified camera with an extended blue response was fitted with a broad band filter to observe the N_{2+} first negative and N2 second positive emissions (band width, 350 475 nm). Novel infrared measurements were made using an InGaAs imaging array operating at video rates. All four cameras had similar fields of view (25°) and were co-aligned on a single mount with the high speed imager. We discovered that sprites were easily imaged in the infrared spectral range, and over 30 events were captured with the InGaAs camera arising from thunderstorms over the mid-western United States during early July and mid August. This poster presents new measurements of the optical characteristics of TLEs imaged in the infrared spectral range (1-1.5 microns) and an initial comparison with their visible and near UV signatures.

Session G1: Banquet Talk

Copper Mill Restaurant
Friday, October 6, 2006 8:30PM - 9:30PM
Chair: Jan Sojka, Utah State University
SPS Student Introduction: Andrew Auman

(8:30) G1.00001: Highlights of NASA's Science Program
Invited Speaker: Mary Cleave

Session H1: Nanoscale Physics

Eccles Conference Center - Room 216
Saturday, October 7, 2006 8:30AM - 10:18AM
Chair: J.R. Dennison, Utah State University
SPS Student Introduction: Ethan Lindstrom

(8:30) H1.00001: Toward Nanoscale Imaging of Biomolecular Systems

Invited Speaker: Jordan Gerton

Biological cells fabricate and assemble molecular building blocks into diverse molecular networks with striking complexity and functionality. As such, they are model integrated nanosystems whose study should yield important information for optimizing specific cellular functions, and for engineering functional synthetic nanosystems. To study biological systems in this context, it is crucial to observe their molecular machinery at work in a physiologically relevant environment. Currently, there are no techniques that can accomplish this.To study these systems at the molecular length scale, we have developed a near-field microscopy technique called tip-enhanced fluorescence microscopy (TEFM) that combines tapping-mode atomic force microscopy (AFM) with confocal fluorescence microscopy. Briefly, a strong axial field is produced at the focus of a laser beam and an AFM probe is positioned into the focus. This creates a localized dipole field at the tip apex, which can strongly excite fluorescence of nearby chromophores. Scanning the illuminated tip over a surface leads to high-fidelity fluorescence images with resolution limited only by the sharpness of the tip. In contrast to AFM, TEFM also provides single-molecule sensitivity and biochemical specificity when combined with fluorescence labeling. We recently demonstrated ∼10 nm resolution in TEFM images of quantum dots in air and we are now working to extend its capabilities to liquid imaging and to improve the resolution yet further by attaching carbon nanotubes to the ends of the AFM tips.

(9:06) H1.00002: Apertureless SNOM imaging of higher density samples

Chun Mu , Chang'An Xie , Jonathan Cox , Ben Mangum , Jordan Gerton – Various efforts in optical microscopy have been devoted to overcome the resolution limit imposed by classical light diffraction. Apertureless NSOM (ANSOM) techniques circumvent this limit by placing a sharp atomic force microscope (AFM) tip in the focus of a laser. In our scheme, a green He-Ne laser beam (λ=543 nm) was introduced into an inverted microscope equipped with a high numerical-aperture objective. A mask was used to produce an axially-polarized evanescent excitation field confined to a near diffraction-limited focus spot. The AFM tip will locally enhance the incident optical intensity. This enhanced field locally excites fluorescence on the sample. High-density quantum dot (QD) samples were dried onto a clean coverslip and then imaged using ANSOM. The fluorescence signal was modulated by a lock-in amplifier to suppress unwanted background from the excitation laser. The technique yielded spatial resolution near 10 nm with an optimized peak-peak oscillation amplitude of ∼30 nm. The signal-to-noise ratio (SNR) of single QD within high-density ensembles was measured and individual particles were still easily resolved ($SNR > 5$) at a density of 14 QDs/μm^2.

(9:18) H1.00003: Functionalization and Metalization of Carbon Nanotube Mats

Jacob Fluckiger , Dustin Lloyd , Lei Pei , Robert Davis – An intriguing mechanical material would be an aluminum / carbon nanotube composite. It could combine the ultra high strength of carbon nanotubes with the ductility and manufacturability of aluminum. We are studying the formation of this metal matrix composite by electroplating aluminum on preformed carbon nanotube structures. In order to induce aluminum growth on the nanotubes, chemical modification of the nanotube surface is required. Surface chemical functionalization was performed by suspension and immersion in a succinic acid bath for the loose nanotubes and nanotube mats respectively. The active surfaces consisting of carboxyl groups should form a stable chemical bonds with the aluminum. Characterization of the chemically functionalized buckypaper by water contact angle and x-ray photo electron spectroscopy (XPS) measurements will be presented. Initial metallization studies will also be presented.

(9:30) H1.00004: Preparation of a dense, vertically-aligned carbon nanotube forest from colloidal iron nanoparticles

David Hutchison , Richard Vanfleet , Robert Davis , Brian F. Woodfield , Juliana Boerio-Goates – We report growth of vertically-aligned carbon nanotube (VACNT) forests from 10nm iron oxide nanoparticles in colloid form instead of the usual sputtering technique. The nanoparticles were suspended in water by sonication and dried onto a 20nm layer of alumina on silicon dioxide. VACNTs were grown by chemical vapor deposition using ethylene, hydrogen, and argon. Dense forests up to heights of 0.5 mm with uniform height have been grown. These structures have been shown by other groups to be useful as field emitters.

(9:42) H1.00005: Separation of Single-Walled Carbon Nanotubes by Density using Isopycnic Fractionation

Michael Clemens , Tobias Hertel – Single-Walled Carbon Nanotubes (SWNT) have attracted a significant amount of attention due in part to their nanoscale size and their optical and electrical properties. Research has shown that these properties can vary drastically with a sub-nanometer difference in SWNT diame-

ters. Recent developments in SWNT synthesis have given rise to research towards the separation and characterization of SWNTs by diameter. I report a separation of SWNTs by diameter, and thus density, through micelle suspension and ultracentrifugation in density gradients prepared with iodixanol and water. The isopycnic layers produced by the ultracentrifugation were extracted using a fractionation method. I measure the degree of separation through absorption spectroscopy and photoluminescence spectroscopy of these fractions.

(9:54) H1.00006: The effects of carbon chain length on nano-crystal structure

Hiram Conley , Uma Maran , Robert Davis , Peter Stang – We have applied 3,6-Bis[*trans*-Pt(Pet_3)$_2$Br]-9,10-bis(didecyloxy)phenanthrene self assembling nanocrystals to various surfaces using Langmuir- Blodgett technique. The long range order of the nanocrystals was then imaged using the atomic force microscope. We observed the formation of lines and mono-layers of the nanocrystals.

(10:06) H1.00007: Nanoscale defect architectures and their influence on material properties

Branton Campbell – Diffraction studies of long-range order often permit one to unambiguously determine the atomic structure of a crystalline material. Many interesting material properties, however, are dominated by nanoscale crystal defects that can't be characterized in this way. Fortunately, advances in x-ray detector technology, synchrotron x-ray source brightness, and computational power make it possible to apply new methods to old problems. Our research group uses multi-megapixel x-ray cameras to map out large contiguous volumes of reciprocal space, which can then be visually explored using graphics engines originally developed by the video-game industry. Here, I will highlight a few recent examples that include high-temperature superconductors, colossal magnetoresistors and piezoelectric materials.

Session H2: Condensed Matter Electronic Properties

Eccles Conference Center - Room 205/207
Saturday, October 7, 2006 8:30AM - 10:18AM
Chair: T. C. Shen, Utah State University

(8:30) H2.00001: Femtosecond transient studies of charge transfer in polymers doped with acceptor molecules; applications for organic solar cells

Josh Holt , Chuanxiang Sheng , Tomer Drori , Z. Valy Vardeny – Current developments in organic solar cells (∼5% efficiency nowadays) require understanding and control of charge carrier transfer and electronic state dynamics of donor-acceptor pairs. One current drawback to organic solar cell efficiency is negligible absorption in the near infrared region of the solar spectrum. We provide evidence that poly(2-methoxy-5(2'-ethyl)hexoxy-phenylenevinylene) (MEH-PPV) doped with 2,7-dinitrofluoronone (DNF) forms a charge transfer complex state that can extend absorption into the near infrared. We found that photoluminescence and the photoinduced absorption (PA) band of excitons are simultaneously quenched. Ultrafast spectroscopic measurements with spectral range from 0.2 to 1.2 eV provide insights into polaron and exciton band dynamics for these complexes. We also suggest a mechanism for bimolecular charge transfer in this system.

(8:42) H2.00002: Optical and Transport studies of isolated and aggregated molecular wires

Alexandre Ndobe , Vladimir Burtman , Golda Hukic , Valy Vardeny – We have studied the optical and transport properties of self assembled monolayer of a mixture of conducting molecules methyl-bezenedithiol (Me-BDT-wire) and non conducting molecules Pentathiol (PT-spacer). The I-V characteristic dependence of the fabricated diodes on the ratio, r of wire/spacers reveals that at low ratio 10-8 $<$ r $<$ 10-3, the transport studies of this mixture can provide us with single molecule resistance of Me-BDT; With the knowledge of the number of conducting molecules which we estimated by multiple self assembly and titration, we found that the single molecule resistance of Me-BDT is 600 MΩ. At high ratio r $>$ 10-4, we found that the conducting molecule tend to aggregate and form a broad resonant state at mid gap that is detectable through the differential conductance measurements as well as by optical absorption and photoluminescence emission.

(8:54) H2.00003: Surface Green function calculations in the infinite number of principal layer approach: A non-recursive scheme

Aleksey Kletsov , Yuri Dahnovsky , Vinz Ortiz – A novel computational method for a surface Green function matrix is determined for the calculation of electrical current in molecular wires. The proposed non-recursive scheme approach allows one to find the imaginary part of the surface Green matrix by the method that includes the infinite number of principal layers. It is shown that the solution of the second order matrix equation gives the spectral density matrix which for noninteracting electrons determines the density of states. Single and double principle layer models are studied both analytically and numerically.

(9:06) H2.00004: Coherent Excitation of the Optic Phonon in Si Measured with Femtosecond Spectroscopy

D.M. Riffe , A.J. Sabbah – Using 28 fs, 800 nm laser pulses from a Ti:sapphire oscillator we have coherently excited, and subsequently probed with time dependent reflectivity, the Si zone-center optic phonon. The reflectivity modulations are well described by an underdamped oscillator $(\Delta R/R)\exp(-t/\tau)\cos(2\pi t/T+\phi)$ with amplitude $\Delta R/R \approx 5\times10^{-6}$, phase $\phi = 86 \pm 14$ degrees, period $T = 64.07 \pm 0.07$ fs, and decay time $\tau = 2.75 \pm 0.15$ ps. The phase indicates that transiently stimulated Raman scattering (TSRS) is responsible for the coherent-phonon generation: our result are in good agreement with a recent theory of TSRS for opaque materials [T. E. Stevens *et al.*, Phys. Rev. B **65**, 144304 (2002)] when we extend the theory to include the finite lifetime of the excited charge density that drives the oscillation. Additionally, the period and decay time of the coherent oscillations are consistent with carrier-density dependent Raman-scattering measurements.

(9:18) H2.00005: Electron transport in laterally confined phosphorus δ-layers in silicon

S.J. Robinson , J.R. Tucker , T.-C. Shen – Carrier transport in 1D semiconductor structures has not been much studied experimentally because of the difficulty of confining dopant atoms in a quasi-1D configuration in a crystal. In the past few years we have developed a UHV-STM-based fabrication scheme to create 2D nanoscale patterns buried in crystalline silicon. By selectively desorbing H from a Si surface and dosing the dangling bonds with PH_3, we can create laterally confined conductive P δ-layers with widths on the order of 10 nm. These nanowires are connected to arrays of As-implanted contacts for transport characterization. Electrical measurements at cryogenic temperatures show ohmic behavior and magnetoconductance in accordance with weak localization theory. In addition, by lowering the temperature continuously, we find a clear 2D to 1D transition as the phase coherence length approaches the wire width. In 1D, the nanowire resistance becomes independent of temperature, indicating a saturation of the phase coherence and thermal lengths due to inelastic boundary scattering in the wire. Large-scale integration of δ-layer devices and potential 3D architectures will become possible by employing the UHV-photolithography currently

under development.

(9:30) H2.00006: Calculation of efficiency losses in Cu(In,Ga)Se2/CdS solar cells with ultra-thin absorbers

Ana Kanevce , James Sites – One of the main obstacles for commercialization of solar cells based on Cu(In,Ga)Se2 absorbers is the price and unavailability of indium. An obvious way to reduce the amount of indium required is to reduce the thickness of the Cu(In,Ga)Se2 absorber. This work uses numerical simulations to investigate the physical aspects of the changes that should occur with thinner absorbers. As the thickness becomes smaller than the diffusion length, the back-contact recombination losses increase. Increased Ga content towards the back contact can improve the carrier collection and lower the recombination loss. The influence of Ga/In distribution throughout the absorber and the necessary Ga/In ratio are calculated. The effect of nonuniformities on the solar cell behavior has been investigated, with emphasis on comparison between thinner (below 500 nm) and thicker (1 micron and above) devices. Devices thinner than 500 nm are less forgiving to thickness nonuniformities than the thicker ones. Band-gap nonuniformities cause collection problems and lower the fill-factor.

(9:42) H2.00007: E-Field Conditioning and Charging Memory in Low Density Polyethylene

Jerilyn Brunson , J.R. Dennison – Accurate measurement of electronic properties in extremely high resistivity materials must take into account a number of ways in which the measurements influence the materials properties being probed. These can include the strength of the applied electric field, the number of successive exposures to an applied field, the duration of exposure, and recovery time allowed during exposure cycles. An extensive series of constant voltage measurements of the resistivity of low density polyethylene samples were taken to determine consistency of measured resistivity results, the effects of varying electric field amplitude, and the extent of charging memory. Higher electric fields were found to lower the resistivity, as predicted by hopping conductivity models of polymers. Measurements at a particular voltage showed that the dark current resistivity approach successively lower values with repeated exposure.

(9:54) H2.00008: Electric Field Induced Hopping Conductivity: An Investigation of Electric Field-Dependent Resistivity in Polymers

S.R. Hart , J. Brunson , J.R. Dennison – The resistivity of highly insulating materials exhibits a dependence on electric field strength. Mott and Davis as well as Poole and Frankle describe theoretically the resistivity of disordered semiconductors, when subject to a changing electric field, in terms of hopping conductivity models. While these models have often been applied to polymers, there is little direct experimental evidence to confirm the validity of the theories for polymers. We present such results for a newly-developed block co-polymer Hytrel, a highly insulating material similar to Teflon. The constant voltage resistivity test method has been used to study Hytrel for a range of electric fields up to electrostatic breakdown. We consider whether the Hytrel results are consistent with existing models of electric-field induced hopping conductivity.

(10:06) H2.00009: Photodarkening of Te-modified TiO2 Nanocrystals

Steven Phillips – The photocatalytic properties of TiO2 nanocrystals can be enhanced by doping, which can result in increased absorption in the visible range. After annealing Te-modified TiO2 nanocrystals, the powder becomes photo-sensitive, changing from an off-white color to a dark-red color under UV and visible illumination. This color change is stable, but can be reversed by annealing the powder again. We analyze the nanocrystals with x-ray diffraction, x-ray photoelectron spectroscopy, electron spin resonance, and transmission electron microscopy. Currently, the main question we are investigating is whether the Te is in the interior of the nanocrystals or on the surface.

Session H3: Applied Physics and Spectroscopy

Eccles Conference Center - Room 201/203
Saturday, October 7, 2006 8:30AM - 10:18AM
Chair: Charles Durfee, Colorado School of Mines

(8:30) H3.00001: Near-field mapping of pressure fields during active noise control of small axial cooling fans

Benjamin Shafer , Cole Duke , Kent Gee – In the past, tonal noise from small axial fans has been globally reduced using active noise control (ANC) with near-field error sensors placed according to a theoretical condition of minimized radiated power [K.L. Gee and S.D. Sommerfeldt, J. Acoust. Soc. Am. **115**, 228-236 (2004)]. The theoretical model, based on mutual coupling of point sources, showed that pressure nulls exist in the near field when the total radiated power is minimized. Error sensor placement at these locations should then optimize global ANC. This study comprises an experimental investigation in which the actual locations of these near-field pressure nulls have been measured over a two-dimensional grid with a linear array of microphones. The array consists of 25 quarter-inch microphones with half-inch spacing. This array has been used to map the radiated pressure field from a 60mm cooling fan during ANC, in addition to a benchmark case, where a small loudspeaker has been mounted in place of the fan. The experimental results are compared to the theoretical pressure null locations in order to determine the efficacy of the point source theoretical model.

(8:42) H3.00002: Use of near-field energy-based error signals for active control of free-field sound

Ryan Chester , Timothy Leishman – Practical efforts to actively control sound often require error sensors located in the acoustic or geometric near field of sound sources. Conventional pressure-based error sensors are highly sensitive to near-field position and other system parameters due to the spatial and spectral variation of the pressure field. Other acoustic quantities are less sensitive to spatial and spectral changes. This paper compares the potential, kinetic, and total energy density in the near field of sound source pairs. It also discusses the spatial and spectral variations of the aforementioned quantities.

(8:54) H3.00003: The Effects of Nonlinear Propagation on Acoustic Source Imaging in One-Dimension

Micah Shepherd , Kent L. Gee – The acoustics of finite-amplitude (nonlinear) sound sources, such as rockets and jets, are not well understood. Characterization of sound pressure amplitudes, aeroacoustic source locations and frequency dependence of these sources is needed to assess the impact of the acoustic field on the launch equipment and surrounding environment. Nonlinear propagation of high-amplitude sound is being studied to determine if a source-imaging method called near-field acoustical holography (NAH), which is based on linear assumptions, can be used to estimate the source information mentioned. A one-dimensional numerical algorithm is being used to linearly and nonlinearly propagate the radiation from a monofrequency source. NAH is used to reconstruct the source information from the simulated data and the error is determined in decibels.

(9:06) H3.00004: Aerodynamic and Propulsion Assisted Maneuvering for Waverider Vehicles

Patrick Jolley – Waveriders have long been sought after as the ideal space vehicle for space based aero assist maneuvers. Theoretically, waveriders can significantly increase gravity assist missions by performing an aero assist maneuver. These maneuvers are possible due to their high lift over drag ratio. However, implementing the theory is more difficult when considering the actual flight aerodynamics and heating problems that will be encountered. An aerodynamic database was generated using hypersonic incidence angle analysis tools with a viscous skin-drag correction. A performance analysis is performed and analyzes stagnation point heating, handling qualities, and controllability, etc. Finally, a simulation is being built to analyze various trajectories and possible mission scenarios.

(9:18) H3.00005: Flush Air Data Sensing System for Trans-Atmospheric Vehicles

Joel Ellsworth – With the emergence of multiple companies attempting to tap the space tourism market, as well as NASA's return to the moon initiative, an inexpensive but reliable means of determining wind relative vehicle attitude is becoming a necessity. The traditional means of obtaining air data (altitude, Mach number, angles of attack and sideslip) using fixed pitot probes and directional flow vanes is not viable for collecting data on high supersonic and hypersonic vehicles, due to the high temperatures and dynamic pressures. The solution is to use a matrix of flush mounted pressure ports on the vehicle nose or on an outboard wing leading edge. Since the ports will be located behind a detached shock wave at supersonic velocities, the temperatures will remain substantially lower. A Flush Air Data Sensing (FADS) system can also be used for subsonic conditions, although it must be calibrated for the effects of the vehicle geometry. The physics of air behavior and the mathematics of the solution algorithm will be presented. Several relevant examples of planned vehicles will be presented. [

(9:30) H3.00006: Conical soft x-ray Von Hamos spectrometer

Matthew Harrison , John E. Ellsworth , Alexander Shevelko , Larry V. Knight – The soft x-ray spectroscopy group has designed and implemented a unique form of the Von Hamos spectrometer. Von

Hamos spectrometers are used to provide spectral information of laser produced plasmas, and commonly have a detector placed perpendicular to the focusing plane. Such a set up provides a large spectral range at high resolution, but does not allow for absolute intensity information. This new design places our CCD detector parallel to the focusing plane, allowing for the absolute calibration of the plasma source.

(9:42) H3.00007: Conical Reflection in Direct Simulation Monte Carlo

Andrew Sampson , Adam Payne , William Somers , Ross Spencer – Fenix is a particle-in-cell simulation, using a Direct Simulation Monte Carlo method, and is aimed to improve the accuracy of Inductively Coupled Plasma Mass Spectrometry (ICP-MS). It currently focuses on the ICP-MS first expansion region through a supersonic nozzle in cylindrical symmetry. Due to increased complexity in Fenix, it has become necessary to solve the general conical surface reflection problem. The previous method, the new solution, and results from the enhanced simulation will be presented.

(9:54) H3.00008: Increasing Diagnostics Resolution in a Monte Carlo Simulation of an ICP-MS

Adam Payne , Andrew Sampson , William Somers , Ross Spencer – An implementation of the Direct Simulation Monte Carlo Method has been used to model the physical behavior of plasma gas in an Inductively Coupled Plasma mass spectrometer as it expands supersonically through a nozzle. As the simulation proceeds, data is taken over prescribed cells and then averaged to determine steady state physical properties such as temperature, density, and velocity. Special attention is given to plasma flow through the nozzle. Results from multiple simulations which show high resolution images of the plasma properties inside the nozzle are presented.

(10:06) H3.00009: Supersonic Nozzle Flow Using DSMC

William Somers , Adam Payne , Andrew Sampson , Ross Spencer – Fenix is a particle-in-cell Direct Simulation Monte Carlo (DSMC) computer simulation which models gas flow through an inductively coupled plasma mass spectrometer (ICP-MS). Particular attention is given to a nozzle region in the ICP-MS where gasses moving through a steep pressure gradient undergo a supersonic transition, expanding into a near vacuum environment. The physical behavior of the gasses in the nozzle region are closely studied, including interaction with the thermalized nozzle, incompressibility of the gas, and flow fields near the nozzle. Fenix has recently reached a stage of completion allowing our research group to produce pressure, temperature and velocity flow data for various regions in the ICP-MS. It is now necessary to verify the algorithms used in Fenix, and to check our work against other methods. Grahame Bird, one of the foremost experts in DSMC simulations, has made available to the public a general DSMC simulation which may be used to model the ICP-MS. Bird's simulation will be used to corroborate the data produced by Fenix, and the images of flow conditions for each method will be presented and compared.

Session H4: Fields and General Theory

Eccles Conference Center - Room 305
Saturday, October 7, 2006 8:30AM - 10:06AM
Chair: Charles Torre, Utah State University

(8:30) H4.00001: Possible origin of inertial mass and of De Broglie wave

Alexander Panin – Inertial mass naturally originates in the system of standing relativistic waves (i.e., waves moving with the same speed c in any reference frame) - just as a by-product of Lorentz transformations between observer's and standing wave's reference frames. Another mathematical by-products are origination of De Broglie wavelength (of the standing wave packet), of the second Newton law (in correct relativistic form), and of least action principle. So it is possible that everything in our universe (=all "elementary" particles we know) consists of only one object - relativistic wave moving with only one speed - c. Mathematical details are presented in the paper.

(8:42) H4.00002: Special relativity: two postulates or one?

David Eckhard , Alexander Panin – In current physics textbooks special relativity is derived from Einstein's two postulates: 1.The laws of physics are the same in all inertial frames. 2. The speed of light is the same as measured in all inertial frames. Because the speed of light is also the proportionality constant in the strength of electromagnetic interactions, and is among three fundamental constants (c, h, G) governing laws of physics, then the second postulate is the consequence of the first one (indeed, otherwise Coulomb law and all e/m phenomena would be reference frame dependent). Therefore, should not SR be reduced to one postulate only? Details of this discussion are presented.

(8:54) H4.00003: Causality in Classical Electrodynamics: a Comparison of Different Approaches

Himal Rathnakumara , Manuel Berrondo – Causality for classical charged particles has been traditionally interpreted in terms of the retarded solution of Maxwell's equations. Combined with the Lorentz equation, radiation reaction for point particles produces runaway solutions. On the other hand, Feynman's propagator implies causality in terms of the proper time of the particle and is hence compatible with classical electrodynamics where proper time and the time coordinate flow in the same direction. In this work, we propose to find the radiation reaction equation for a classical point charged particles assuming causality in the Feynman-Stuckelberg sense with the aid of the Clifford algebra formalism. We provide a comparison of methods which will give insight into the solution.

(9:06) H4.00004: Performance requirements for ensemble implementations of quantum algorithms

David Collins – We consider the statistical performance of quantum algorithms when implemented on ensemble quantum computers. In particular we consider an ensemble quantum computer initially in a pseudopure initial state and determine the minimum polarization needed so that the quantum algorithm outperforms classical probabilistic competitors. We propose a general method for finding the minimum polarization and apply it to single bit output algorithms such as the Deutsch-Jozsa algorithm and the multiple output bit Grover search algorithm.

(9:18) H4.00005: Isometric Families of Minimal Surfaces

Stephen Taylor – We consider a minimal surface M immersed in R^3 with induced metric $g = \psi\delta_2$ where δ_2 is the two dimensional Euclidean metric and 2ψ is a scalar. We then construct a system of partial differential equations that constrain M to lift to a minimal surface via the Weierstrauss- Enneper representation demanding the metric is of the above form. It is concluded that associated surfaces connecting the prescribed minimal surface and its conjugate surface satisfy the system. Moreover, we find a non-trivial symmetry of the system that generates a one parameter family of surfaces isometric to a specified minimal surface. We demonstrate an instance of the analysis for the catenoid ($\psi = \cosh^2(v)$), and comment on potential generalizations to a Lorentzian manifolds in a general relativistic setting.

(9:30) H4.00006: Stability of D1/D5 Black Strings

Jared Greenwald , Eric Hirschmann – We are interested in the stability of black strings. In particular, we are investigating the Gregory-Laflamme instability for a broader class of black strings. We consider a model from low energy string theory in six dimensions, often referred to as the D1/D5 system. In an effort to analyze this system, we investigate the stability of the corresponding black string through perturbative methods. We describe a solution with non-constant dilaton and then sketch the perturbation method and our numerical scheme for finding indications of instability.

(9:42) H4.00007: Kaluza-Klein Masses and Couplings: Radiative Corrections to Tree-Level Relations

Sky Bauman – The most direct experimental signature of a compactified extra dimension is the appearance of an infinite tower of Kaluza-Klein particles. For example, a single flat extra dimension compactified on a circle leads to Kaluza-Klein states whose masses are integral multiples of the compactification scale and whose couplings are independent of the mode number. However, these masses and couplings are subject to radiative corrections. In this talk, I investigate the extent

to which such radiative corrections deform the expected tree-level relations between Kaluza-Klein masses and couplings. As toy models for our analysis, I investigate a five-dimensional scalar ϕ^4 model and a five-dimensional Yukawa theory involving both scalars and fermions. In each case, I identify the conditions under which the tree-level relations are stable to one-loop order, and the situations in which radiative corrections distort these relations by introducing entirely new dependences on mode number. One unexpected result is that the squared masses of the fermions in Yukawa theory receive corrections that actually grow with mode number. Another is that a γ^5 interaction is radiatively induced in this theory. Although small, such corrections to the Kaluza-Klein spectrum can therefore distort the measurement of the apparent geometry of a large extra dimension, and may be observable at future colliders. Along the way, I also develop several new calculational techniques for renormalization in higher dimensions.

(9:54) H4.00008: Effects of Dynamical Compactification on D-Dimensional Gauss-Bonnet FRW Cosmology

Keith Andrew , Brett Bolen , Chad Middleton – We examine the effect on cosmological evolution of adding a string motivated Gauss-Bonnet term to the traditional Einstein-Hilbert action for a (1 + 3) + d dimensional Friedman-Robertson- Walker (FRW) metric. By assuming that the additional dimensions compactify as the usual 3 spatial dimensions expand, we find that the Gauss Bonnet terms give perturbative corrections to the FRW equations. We find corrections that appear in the calculation of both the Hubble constant, H0, and the acceleration parameter, q0, for a variety of cases that are consistent with a dark energy equation of state.

Session H5: Atmospheric and Nuclear Physics

Eccles Conference Center - Room 309
Saturday, October 7, 2006 8:30AM - 10:06AM
Chair: Andrea Palounek, Los Alamos National Laboratory

(8:30) H5.00001: Propagation and Ducting of Short-Period Gravity Waves over Antarctica

Kim Nielsen , Michael Taylor , Robert Hibbins , Martin Jarvis– Short-period gravity waves are known to be significant sources of momentum deposition in the upper mesosphere. Recent studies using an extensive imaging data set obtained as part of a collaborative program with British Antarctic Survey have identified significant momentum transported by short-period waves as observed from Halley Station (76 $^{\circ}$S,) on the Brunt ice shelf. However, this result is recognized to be an upper limit since it assumes that all of the wave motions were freely propagating. In this study we utilized available mesospheric wind data from Halley to investigate the propagation nature (i.e. freely propagating, evanescent, or Doppler ducted) of these waves observed over Halley during the 2000 and 2001 austral winter seasons to help provide a more realistic assessment of the impact of short-period waves on the Antarctic environment. A total of $\sim$170 short-period wave events were observed with available coincident wind measurements. The majority of these waves were found to be freely propagating ($\sim$76%) with only $\sim$2% of the observed events clearly Doppler ducted. In the remaining cases (22%), the mesospheric winds did not support propagating waves (evanescent).

(8:42) H5.00002: Imaging Gravity Waves and Sprites in the Earth's Upper Atmosphere

Michael Taylor – Ground-based remote sensing studies of the Earth's upper atmospheric regions provide a low-cost and reliable method for long-term measurements. At mesospheric heights ($\sim$60-100 km) the atmospheric pressure and density are lower than can be achieved in most vacuum systems yet this tenuous region is home to a wealth of dynamical phenomena. In particular atmospheric gravity waves, generated by thunderstorms, severe weather, and by strong winds blowing over large mountain ranges (such as the Rockies), can propagate upwards from their source regions into the mesosphere in only a few hours. At heights above about 80 km these waves start to break (like ocean waves as they reach the shore) and deposit their energy and momentum which has a dramatic influence on the upper atmospheric circulation and the temperature field. We use sensitive CCD imaging systems to characterize these gravity waves and much larger-scale tidal perturbations using the naturally occurring nightglow emissions. Currently we have cameras operating remotely in Utah, Hawaii, Antarctica (and soon in Norway), to help study their global variability and dominant source regions. This talk will introduce the topic of atmospheric imaging with examples of our current research. Novel applications of imaging techniques to other areas of our ongoing atmospheric research will also be presented.

(8:54) H5.00003: Three New Ionospheric Indices

Cesar Noguera , Jan Sojka – In the present work three new ionospheric indices have been proposed as an exploratory way to quantitatively evaluate the ionosphere state. These indices have been determined from a statistical analysis of ionosphere GPS total electron content (TEC) measurements that were assimilated into the USU global assimilation of ionospheric measurements (GAIM) model. Comparisons of the indices from 8 locations demonstrate both local and regional value of these indices. A correlation study has been performed between the new indices and others such as kp, Dst and F10.7 which shows that the ionosphere's variability can not be specified by these solar and geomagnetic indices. Hence we put forward the concept that a GPS TEC index is the appropriate means of describing regional ionospheric variability.

(9:06) H5.00004: Extracting air motion velocity data from aerosol distortion patterns detected in fast lidar scans

Jan Marie Andersen , Thomas Wilkerson – Rapid elevation scans using a LIDAR pointing in the upwind direction at a fixed azimuth reveal distinct patterns in the spatial structure of the aerosols in the low-altitude boundary layer. Typically, these aerosol clouds are borne aloft from air pollution sources and areas of loose soil such as gravel roads and plowed fields. Such aerosol patterns are kinematically distorted due to the combination of finite scan time and cloud motion. True motion patterns are interpreted by means of a joint analysis of successive "up" and "down" scans. Analysis of two fast, successive elevation scans yields information about the motion of the cloud features and the fluid flow of the air itself - and thus about the turbulent motion within the atmospheric boundary layer. In spite of scan limitations, the temporal and spatial dependence of air flow can be determined by careful analysis of these repeated pairs of rapid scans. Examples are given of measurements of the mean horizontal wind, the shape of prominent vertical plumes of wind-borne aerosols, and inferences about vertical aerosol transport.

(9:18) H5.00005: Heavy Baryons at CDF II

John Ash – We describe heavy baryon production and decay produced at the Tevatron and recorded by the CDF detector during Run II. Motivation for studying heavy baryons is given. We describe how the collider, detector, and trigger work together to produce meaningful data. Results are then compared against recent theoretical predictions.

(9:30) H5.00006: Influence of the Ground State Spin of the Projectile -target on the Fission Anisotropies

Aziz Bhkami – Fission fragment angular distributions have been investigated for various systems produced in heavy ion reactions at near and sub-barrier energies. In particular, special attention has been paid to the entrance channel dependence of fragment angular distributions. The results of our analysis of the fragment angular anisotropies induced by Boron, Carbon, and Oxygen ions on Thorium and Neptunium targets as well as Fluorine ions on Neptunium target indicate that at bombarding energies around fusion barrier the Transition State Model (TSM) is quite successful in accounting for the observed angular distributions. We have further found that the fission anisotropies strongly depend on the channel spin in consistence with the prediction of the pre-equilibrium model.

(9:42) H5.00007: Proton configuration and mass variations are observed in each of the 3036 isotopes studied.

Eugene Pamfiloff – The fission and decay transitions of unstable isotopes are studied with particular detailed analysis of nuclei masses, proton - neutron substructure, and the change in mass experienced by individual nucleons of parent, daughter and product isotopes. The data shows the 3036 isotopes studied contain nucleons of a mass unique to each isotope, and further, indicating 3036 proton variations, each differentiated by a distinct mass. Of these, 283 proton variations are further distinguished by belonging to stable benchmark isotopes. The same variations were found with bound neutrons. A direct correlation is observed between the nearest stable benchmark mass and the mass of the nucleon returning to ground state during the transition, indicating a mass dependence to nuclear stability. These findings indicate that a nucleus in an excited state cannot stabilize or return to the ground state until it adjusts mass to match the nearest $Z - N$ and mass per nucleon benchmark. These conclusions were further tested with the analysis of nucleon mass adjustments occurring within the natural and artificial alpha emitter nuclei. The developed system of analysis provided good results when tested against the incident and product particles of high and low energy interactions and events of nuclear transmutation. Every transition to a stable product demonstrates a strong correlation with a specific mass per nucleon benchmark as a third condition of nuclear stability.

(9:54) H5.00008: Accelerate the transition of radioisotopes and unwanted weapons-grade ^{239}Pu into stable nuclei with a system of high frequency modulation for a net energy gain

Eugene Pamfiloff – A process of high frequency stimulation of nucleons can be utilized for the accelerated fission, decay or controlled transition of unstable isotopes. ^{238}U could be persuaded to transition promptly into the stable ^{206}Pb isotope, where a portion of the total mass difference of 29873.802 MeV per nucleus becomes available energy. The proposals of this paper describe an effective system for nuclei stimulation configured to accelerate such a series of 14 transitions over several milliseconds, instead of 4.47 x 10^9years. Positive ions or ionized capsules of fuel suspended by magnetic fields and subjected to the system of correlated frequency modulation of multiple beam lines, tailored to the specific target, will emit sufficient energy to stimulate subsequent targets. The system can be applied to all radioisotopes, nuclear waste product isotopes such as ^{239}Pu, and a variety of other suitable unstable or stable nuclei. Through the proposed confinement system and application of high frequency stimulation in the 10^{22} to 10^{24} Hz regime, the change in mass can be applied to both the fragmentation of subsequent, periodically injected targets, and the production of heat, making a continuous supply of energy possible. The system allows the particle fragmentation process to be brought into the lab and provides potential solutions to the safe disposal of fissile material.

Session I1: The Final Frontier?

Eccles Conference Center - Room 216
Saturday, October 6, 2006 10:45AM - 12:33AM
Chair: Keith Dienes, University of Arizona
SPS Student Introductions: Sydney Chamberline, Thomas Williams, Jodie Tvedtnes

(10:45) I1.00001: What's New in Gravitational Physics
Invited Speaker: Charles Torre
For nearly a century Einstein's General Theory of Relativity has provided our best theory of space, time, and the gravitational interaction. In 2006, research in gravitational physics is, in many ways, at an unprecedented level of activity. In this talk I will give a superficial survey of some of the current hot topics in gravitational physics research. I will emphasize: current and future gravitational wave searches, the 2-body problem in general relativity, and approaches to constructing a quantum theory of gravity.

(11:21) I1.00002: Gravitational Holography
Invited Speaker: Scott Thomas
The asymptotic number of states in an appropriately defined region in any theory of quantum gravity which reduces to Einstein gravity at large distances is equal to one quarter of the area in Planck units. A non-redundant description therefore requires only a hologram at the boundary of the region. The holographic properties of the states in quantum gravity lead to a mixing of the usual concepts of ultraviolet and infrared. This mixing is at odds with various properties of local quantum field theory such as the Heisenberg uncertainty relation as well as the upper bound on the fixed angle inclusive cross section in very high energy collisions. The holographic properties of gravity also imply that quantum contributions to the vacuum energy are finite and parametrically at most of order the classical value from which the infrared curvature scale is determined. Gravitational holography therefore provides a technically natural solution to the cosmological constant problem which plagues any local quantum field theory description of gravity.

(11:57) I1.00003: Quantum Universe
Invited Speaker: Hitoshi Murayama
What is the Universe made of? How did it come to be? Why do we exist? This kind of fundamental questions about the Universe used to be just philosophy, but are now coming into the realm of quantitative science. The key is in quantum physics of elementary particles that determined the evolution of the Universe when it was very young. I will discuss this amazing connection between the large (the Universe) and the tiny (elementary particles), in the context of current and forthcoming experiments.

Session SA: Student Awards

Eccles Conference Center - Room 216
Saturday, October 6, 2006 12:35PM - 12:45PM
Chair: Keith Dienes, University of Arizona

Presentations of the awards for the best student talks and posters will be made.

Author Index

—- A
Abbott, J. F1.19, F1.20
Abbott, Jonathan B2.6
Abel, Joseph F1.29
Adak, Sourav F1.11
Adams, Daniel B2.1
Adams, Mark B2.2
Addae-Kagyah, Michael D3.5
Agosta, Dennis F1.25
Al Khatatbeh, Yahya B3.5
Albretsen, Jennifer F1.31
Alenazi, Moqbil B4.4
Allred, David F1.6, F1.38
Andersen, Jan Marie H5.4
Andreev, Alexandre V. F1.30
Andrew, Keith H4.8
Ansaldo, E.J. B3.3
Archibald, James B2.9, F1.26
Armstrong, John F1.5
Arnold, Michelle D2.4
Ash, John H5.5
—- B
Bailey, Matt F1.40
Baker, Ian F1.31
Balasubramaniam, K. F1.4
Barnett, Katherine F1.37
Barton, Sarah B2.4
Bauman, Sky H4.7
Benitez-Medina, Julio Cesar F1.34
Bera, Sudipta B2.1
Berrondo, Manuel H4.3
Bhattacharya, Tanmoy B1.1
Bhkami, Aziz H5.6
Birrell, Jeremiah F1.16
Bishop, Jeremy D3.8, F1.9
Boerio-Goates, Juliana H1.4
Bolen, Brett H4.8
Bowman, Gary D4.1
Brueck, E. B3.3
Brimhall, Nicole B2.2, B2.3
Brimhall, Niki F1.6
Brunson, J. H2.8
Brunson, Jerilyn H2.7
Burk, Laurel D1.2
Burtman, Vladimir H2.2
—- C
Campbell, Branton D1.8, H1.7
Carroll, Bradley D4.8
Cary, John B1.2
Chester, Ryan H3.2
Childress, Colby B2.1
Christensen, Dan D4.2, F1.16
Christiansen, Eric B2.2
Cleave, Mary G1.1
Clemens, Michael H1.5
Cobble, J. F1.18
Coburn, James D4.7
Collins, David H4.4
Conley, Hiram H1.6
Cook, Shon F1.32
Corbridge, J. F1.19, F1.20
Cox, Brady D1.3
Cox, Jonathan H1.2
Cullen, David B3.9
Cummer, Steven F1.40
—- D
Dahnovsky, Yuri H2.3
Davies, Rob B2.6
Davis, Robert D1.2, H1.3, H1.4, H1.6
Davis, Robert C. F1.37
DeLand, Matthew F1.1
Dennison, J. D1.1
Dennison, J.R. B2.6, B2.7, B2.8, F1.19, F1.20, F1.21, H2.7, H2.8
Devolder, B. F1.18
Doak, R.B. D2.1, D2.2
Doermann, Greg F1.26
Doyle, Timothy D2.5
Drori, Tomer H2.1
Duke, Cole H3.1
Durfee, Charles B2.1
Durfee, Dallin B2.9, D4.2, F1.16, F1.26
—- E
Eckhard, David H4.2
Edwards, Farrell F1.9
Edwards, W.F. D3.9, F1.8
Edwards, William D3.8
El-Khatib, Sami B3.2, B3.3
Ellsworth, Joel H3.5
Ellsworth, John E. B4.1, B4.2, D3.6, H3.6
Erickson, Christopher F1.16, F1.26
Esquivel, Michael F1.7
Everett, Addison D1.6, F1.27, F1.29
Everett, E. Addison D1.7, F1.39
Everett, Edward D1.5
—- F
Field, Jeff B2.1
Fluckiger, Jacob H1.3
—- G
Gee, Kent H3.1, H3.3
Gerton, Jordan H1.1, H1.2
Giraud, Gavin B2.2
Gondolo, Paolo B4.4
Goyal, Abhijat F1.17
Greenwald, Jared H4.6
Grigg, Amy B2.5, F1.38
Grijalva, C.D. D1.4
Gunther, Jake F1.2
—- H
Hall, Kendy F1.34
Hanna, James F1.31
Hanni, Mark F1.24
Harker, Brian F1.4
Harrison, Matthew H3.6
Hart, S.R. H2.8
Hart, Steve D1.1
Held, E.D. D3.1, D3.2, D3.9, F1.8
Held, Eric D3.4, D3.5, D3.8, F1.9
Herring, T. D1.4
Hertel, Tobias H1.5

Hibbins, Robert H5.1
Hirschmann, Eric H4.6
Hochheimer, Hans D. E1.3
Hodges, J. F1.20
Hodges, Joshua F1.19
Hoffman, N. F1.18
Hoffmann, R.C. B2.6, F1.19, F1.20
Hoffmann, Ryan D1.1, F1.21
Holt, Josh H2.1
Hsu, Bailey B3.8
Huffaker, Diana F1.28
Hukic, Golda H2.2
Humpherys, Candice D4.5
Hunt, A. F1.19, F1.20
Hunter, M. D2.2
Hutchison, David H1.4
—- I
Inglefield, C.E. D1.4
—- J
Jackson, Jacque F1.6
James, John D3.4
Jarvis, Martin H5.1
Jensen, Jerry W. D4.9
Ji, J.Y. D3.1, D3.2
Johnson, Jedediah F1.12
Jolley, Patrick H3.4
Jones, Steven D3.6
Jones, Steven E. B4.1, B4.2
—- K
Kalvius, G. Michael B3.3
Kanevce, Ana H2.6
Karnam, Hema F1.2
Khotapalli, Karunakar F1.30
Kiefer, Boris B3.5, F1.11
Kim, Dong Jun D1.6, D1.7, F1.27, F1.29, F1.39
Kim, Dongjun D1.5
Kite, Jason B2.6, B2.7, B2.8
Kletsov, Aleksey H2.3
Knight, Larry V. H3.6
Knoebel, Jodi F1.37
Komatsu, Shoji B4.5
Kothapalli, Karunakar B3.2
Kullberg, A. D3.9, F1.8
—- L
Laghumavarapu, Ramesh F1.28
Lambert, N. F1.39
Lee, Kanani B3.5
Leishman, Timothy H3.2
Leisure, Robert F1.25
LeRoy, Brian E1.1
Lewandowski, Heather E1.2
Li, Heng D1.4
Llobet, A. B3.3
Llobet, Anna B3.2
Lloyd, Dustin H1.3
Lopez, Jorge A. F1.14
Lyons, Walter A. F1.40
—- M
Malmrose, Michael F1.36
Mangum, Ben H1.2
Maran, Uma H1.6
Martin, Elise F1.12
Mason, Grant D3.7
Mathews, Jay F1.17
Mehta, Manish F1.28
Middleton, Chad H4.8
Mong, Brian B3.6
Morgan, Steven B3.7
Mostafa, Miguel B4.5
Mu, Chun H1.2
Murayama, Hitoshi I1.3
—- N
Nakano, Satoshi B3.4
Nakotte, Heinz B3.2, B3.3, F1.30
Nasreen, Farzana B3.2, F1.30
Ndobe, Alexandre H2.2
Neilsen, David D3.3
Nelson, Nicholas D3.3
Nerdin, Matthew R. B4.1, B4.2
Neyenhuis, Brian B2.9, D4.2, F1.26
Nielsen, Kim H5.1
Noakes, D.R. B3.3
Noguera, Cesar H5.3
—- O
Olijnyk, Helmut B3.4
Ortiz, Vinz H2.3
—- P
Paganetti, Harald D2.3
Painter, John B2.2, B2.3
Palen, Stacy F1.36
Pamfiloff, Eugene H5.7, H5.8
Panin, Alexander H4.1, H4.2
Paul, Justin F1.16
Pautet, Dominique F1.40
Payne, Adam H3.7, H3.8, H3.9
Peak, David D4.6
Peatross, Justin B2.2, B2.3
Pei, Lei H1.3
Phillips, Steven H2.9
Planchon, Thomas B2.1
Plimpton, Steve B1.3
Powell, Melissa D3.7
Powers, Nathan B2.2
Pyper, Brian D4.4, D4.5
—- Q
Qamar, Shahid D2.6
—- R
Rathnakumara, Himal H4.3
Riffe, D.M. H2.4
Rivera, Felipe D1.2
Robertson, Daniel D2.3
Robinson, S.J. H2.5
Rodriguez, Douglas B4.7
—- S
Saam, Brian B3.7
Sabbah, A.J. H2.4
Sampson, Andrew H3.7, H3.8, H3.9
Sandoval, Luis M. F1.14, F1.30
Schirmer, Daniel F1.35
Seco, Joao D2.3
Shafer, Benjamin H3.1
Sharma, M. D3.2
Shen, T.C. F1.33, H2.5
Sheng, Chuanxiang H2.1
Shepherd, Micah H3.3
Shevelko, Alexander H3.6
Shinn, Neal A1.2
Simkhada, Deepak F1.3

Singh, Ajay D3.8, F1.9
Sites, James H2.6
Smidt, Joseph B4.3
Sojka, Jan F1.4, H5.3
Solomon, Stanley C. A1.1
Somers, William H3.7, H3.8, H3.9
Spaulding, R. F1.19, F1.20
Spence, J.C.H. D2.2
Spencer, Ross D3.7, D4.2, H3.7, H3.8, H3.9
Squier, Jeff B2.1
Stang, Peter H1.6
Stockwell, Robert F1.3
Strein, Liz F1.38
Stronach, C.E. B3.3
Swainsson, Ian B3.2
—- T
Tadigadapa, Srinivas F1.17
Takemura, Kenichi B3.4
Tang, Rebecca F1.16
Tanner, Michael B3.9
Taylor, Michael F1.1, F1.3, H5.1, H5.2
Taylor, Michael J. F1.40
Taylor, Mike F1.2
Taylor, P.C. D1.4
Taylor, Stephen H4.5
Thomas, Anthomas D1.1
Thomas, Scott I1.2
Thompson, Shem D4.4
Tiernan, Bill D4.3
Tierney, T. F1.18
Tolle, Charles R. F1.15
Torre, Charles I1.1
Trefilova, Anna F1.23
Trofimov, Alexei D2.3
Tucker, J.R. H2.5
Turley, R. Steven B2.3, B2.4, F1.12
Turley, Steve B2.5
Turner, Brendan F1.28
Turner, John A. A1.3
Turner, Matt B2.2
Turner, Matthew B2.3
Tvedtnes, Jodie F1.1
—- V
Van Huele, Jean-Francois B3.8
van Zijll, Marshall F1.26
Vanfleet, Richard B3.9, D1.2, H1.4
Vardeny, Z. Valy H2.1, H2.2
Vue, Vayee D1.8
—- W
Walch, Shannon B4.1, D3.6
Walker, Gary B4.6
Ware, Michael B2.2, B2.3
Warner, J. D2.2
Warnick, Keith D2.5
Warnick, Keith H. F1.15
Warnick, Sean B2.9
Washburn, Matt F1.26
Washburn, Matthew B2.9
Webb, Michael B3.10
Weierstall, U. D2.2
Weyerman, W. Sam B2.9
Whalen, Dan B4.3
Wheelwright, Heidi F1.33
White, Gary C1.1
Wiencke, Lawrence B4.5
Wilkerson, Thomas H5.4
Wilson, Richard D1.5, F1.27
Wilson, Truman F1.25
Woodfield, Brian F. H1.4
Wright, Matthew B3.1
—- X
Xie, Chang'An H1.2
Xue, Lin F1.13
—- Y
Yang, Haeyeon D1.5, D1.6, D1.7, F1.27, F1.29, F1.39
Yasin, Z. F1.10
—- Z
Zalcik, Mark F1.1
Zeng, Qi F1.31
Zhang, Peng F1.13
Zhang, Qi F1.13
Zhu, Zhihuai F1.13, F1.22